Title

Strategy Evolution in a Skeletal Remodeling and C–H Functionalization-Based Synthesis of the Longiborneol Sesquiterpenoids

Journal

Journal of the American Chemical Society, 144(37)

ISSN

0002-7863

Authors

Lusi, Robert F
Sennari, Goh
Sarpong, Richmond

Publication Date

2022-09-21

DOI

10.1021/jacs.2c08136

Peer reviewed

HHS Public Access

Author manuscript

J Am Chem Soc. Author manuscript; available in PMC 2022 December 05.

Published in final edited form as:

J Am Chem Soc. 2022 September 21; 144(37): 17277–17294. doi:10.1021/jacs.2c08136.

Strategy Evolution in a Skeletal Remodeling and C–H Functionalization-Based Synthesis of the Longiborneol Sesquiterpenoids

Robert F. Lusi[§],

Department of Chemistry, University of California—Berkeley, Berkeley, California 94720, United States

Goh Sennari[§],

Department of Chemistry, University of California—Berkeley, Berkeley, California 94720, United States; Ōmura Satoshi Memorial Institute, Kitasato University, Minato-ku, Tokyo 108-8641, Japan

Richmond Sarpongau

Department of Chemistry, University of California—Berkeley, Berkeley, California 94720, United States

Abstract

Detailed herein are our synthesis studies of longiborneol and related natural products. Our overarching goals of utilizing a “camphor first” strategy enabled by skeletal remodeling of carvone, and late-stage diversification using C–H functionalizations, led to divergent syntheses of the target natural products. Our initial approach proposed a lithiate addition to unite two fragments followed by a Conia-ene or Pd-mediated cycloalkylation reaction sequence to install the seven-membered ring emblematic of the longibornane core. This approach was unsuccessful and evolved into a revised plan that employed a Wittig coupling and a radical cyclization to establish the core. A reductive radical cyclization, which was explored first, led to a synthesis of copaborneol, a structural isomer of longiborneol. Alternatively, a metal-hydride hydrogen atom transfer-initiated cyclization was effective for a synthesis of longiborneol. Late-stage C–H functionalization of the longibornane core led to a number of hydroxylated longiborneol congeners. The need for significant optimization of the strategies that were employed as well as the methods for C–H

Corresponding Authors: **Goh Sennari** – *Department of Chemistry, University of California—Berkeley, Berkeley, California 94720, United States; Ōmura Satoshi Memorial Institute, Kitasato University, Minato-ku, Tokyo 108-8641, Japan;* sennari.go@kitasato-u.ac.jp; **Richmond Sarpong** – *Department of Chemistry, University of California—Berkeley, Berkeley, California 94720, United States;* rsarpong@berkeley.edu.

[§]Author Contributions

R.F.L. and G.S. contributed equally

Supporting Information

The Supporting Information is available free of charge at https://pubs.acs.org/doi/10.1021/jacs.2c08136.

Experimental procedures, spectroscopic data, NMR spectra, and X-ray data for **57** (CCDC 2176918), **58** (CCDC 2176919), and **S8** (CCDC 2191693) (PDF)

Accession Codes

CCDC 2176918–2176919 and 2191693 contain the supplementary crystallographic data for this paper. These data can be obtained free of charge via www.ccdc.cam.ac.uk/data_request/cif, or by emailing data_request@ccdc.cam.ac.uk, or by contacting The Cambridge Crystallographic Data Centre, 12 Union Road, Cambridge CB2 1EZ, UK; fax: +44 1223 336033.

Complete contact information is available at: https://pubs.acs.org/10.1021/jacs.2c08136

The authors declare no competing financial interest.

functionalization to implement these strategies highlights the ongoing challenges in applying these powerful reactions. Nevertheless, the reported approach enables functionalization of every natural product-relevant C–H bond in the longibornane skeleton.

Graphical Abstract

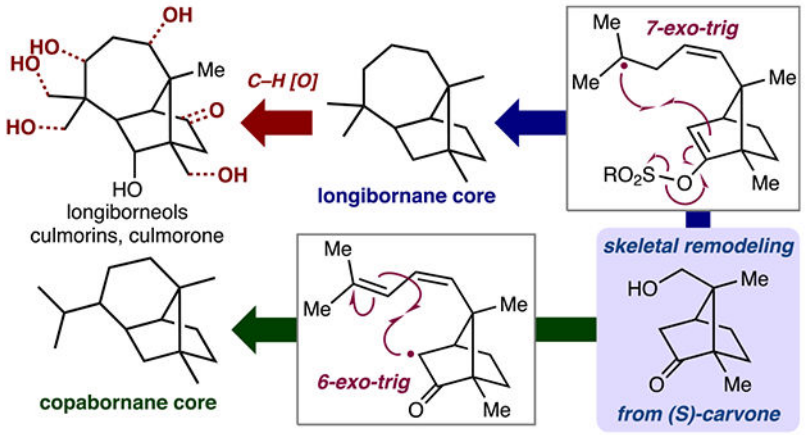

INTRODUCTION

Natural product total synthesis provides an opportunity to test strategies for chemical synthesis and also serves as a proving ground for chemical methods. Recently, two-phase strategies have emerged as a powerful paradigm in divergent syntheses of polycyclic natural products such as terpenoids.[1,2] In such approaches, the carbon framework of a target molecule is constructed in a maximally efficient first phase, after which peripheral functional groups are added in a second phase. By virtue of their topologically complex, polycyclic core, and many oxygenated members,[3–7] the longiborneol family of sesquiterpenoids (e.g., **8**, Figure 1A)[8,9] presented an enticing prospect to highlight such two-phase strategies. In particular, we saw an opportunity to combine two long-standing pursuits of our research group: skeletal remodeling of chiral pool terpenes[10,11] to construct the requisite carbon framework (Phase I) and late-stage diversification through C–H hydroxylation (Phase II).[12,13]

Skeletal remodeling strategies[11] expand the breadth of targets that can be synthesized from the naturally-occurring, chiral terpenes often collectively referred to as the “chiral pool”.[10] Chiral pool terpenes are excellent starting materials in complex molecule synthesis because they are abundant and enable enantiospecific syntheses. Our group has pursued the skeletal remodeling of chiral pool terpenes in order to expand the frameworks that can be accessed from these compounds. Furthermore, we have applied the products of these remodeling efforts as starting materials in several natural product total syntheses (Figure 1A).[11,12,14–16] For example, we have shown that carvone (**1** or *ent*-**1**), which has been used as a starting material in many total syntheses,[10] can be remodeled to camphor derivatives such as 8-hydroxycamphor (**5**).[14] These derivatives represent an intriguing application of skeletal remodeling: the conversion of one chiral terpene framework into another. In this case, a

skeletal remodeling approach allows the preparation of hydroxylated camphor derivatives that would be difficult to prepare by direct derivatization of camphor (Figure 1B).[17] Here, we show that these hydroxylated derivatives of camphor are valuable starting materials for complex molecule synthesis.

Our goal of preparing longiborneol (**8**) from a camphor derivative prompted an aspirational "camphor first" synthesis strategy. Analysis of previous syntheses of natural products that feature bornane subskeletons reveals that the majority construct the [2.2.1]bicycle at a late stage of the synthesis (Figure 2A).[18–23] In our approach, we sought to determine whether an alternative strategy, in which the remainder of the natural product's skeleton is constructed around the [2.2.1]bicycle of a camphor derivative, could yield more efficient syntheses. A late-stage construction of the [2.2.1]bicycle in longiborneol (**8**) is consistent with a retrosynthesis that relies on network analysis[24,25] or a bioinspired retrosynthesis.[26] Of the three syntheses of longiborneol published prior to our work, two use similar strategies. Welch and Waters published a synthesis where the [2.2.1]bicycle is closed using enolate alkylation in step 20 of 21 (Figure 2B).[23] In the shortest previous synthesis of (±)-longiborneol (*rac*-**8**, Figure 2C), Takasu et al. utilized a formal [4 + 2] cydoaddition to construct the [2.2.1]bicycle in step 12 of 16.[22]

Conversely, Kuo and Money synthesized longiborneol using a strategy similar to our proposal (Figure 2D).[27] Beginning from (*R*)-camphor, they synthesized 8-bromocamphor (**18**) in 3 steps and 35% overall yield—although they noted that the sequence was capricious. They installed the remaining carbons of the natural product through an alkylation reaction, and used a key Mukaiyama aldol reaction to close the seven-membered ring and complete the longibomeol framework (see **21** to **22**). While this visionary route demonstrated the feasibility of a camphor-based strategy, it required many functional group interconversions (FGIs), leading to a lengthy synthesis. We posited that skeletal remodeling of carvone could provide access to a complementary camphor derivative that, along with modern chemical methods, would allow us to synthesize longiborneol in fewer steps.

In addition to showcasing the merits of a camphor-based strategy to access longiborneol (**8**), we also saw an opportunity to implement divergent syntheses of its many oxidized congeners (**23**–**32**, Figure 3[3–7]) in a C–H functionalization-based second phase. Because of their relative inertness and ubiquity in organic molecules, the selective derivatization of C–H bonds was once termed a "holy grail" of synthetic organic chemistry.[28] However, many methods to effect such transformations have been developed over the past two decades. Our group has had a long-standing interest in applying C–H functionalization methods in complex molecule synthesis[12–15] in order to circumvent long functional-group-interconversion sequences and to functionalize unactivated positions.[29] These applications test the scope and limitations of C–H functionalization reactions and highlight opportunities for new advancements.[30] Here, using C–H functionalizations in divergent syntheses of the oxidized longiborneol congeners provided the opportunity to use varied methods to diversify a minimally functionalized, C–H rich skeleton.

In this Article, we provide a full account of our synthetic efforts which culminated in a nine-step total synthesis of longiborneol (**8**) from (*S*)-carvone (**1**), as well as syntheses of

eight oxidized longiborneol congeners from a common intermediate.[31] In particular, we detail the evolution of our plan to install the remaining carbon atoms onto a starting camphor framework and to use a subsequent cyclization to form the longibornane scaffold. A reductive radical cyclization intended for this latter purpose led, instead, to a six-membered ring that facilitated a synthesis of copabomeol (**70**, *vide infra*).[32] This observation informed the development of a metal-mediated hydrogen atom transfer (MHAT)-based cyclization to forge the longiborneol framework Additionally, we describe the development of C–H functionalization-based tactics that accomplished late-stage diversification to longiborneol congeners. While several of these functionalization tactics proved ineffective, they provided valuable insight that guided the final routes.

RESULTS AND DISCUSSION

1. Initial Synthesis Strategy.

Our retrosynthesis, outlined in Figure 3, hinged on the assertion that congeners of longiborneol could arise from the parent natural product, or closely related longicamphor (**14**, see Figure 2B), using directed C–H functionalizations (see **33**). While this goal was aspirational, it drove our thinking at that stage of the project. Next, we proposed disconnection of the C6–C7 bond through a cyclization transform, leading back to intermediate **37**. We saw this cyclization as a key challenge of the synthesis. In order to maximize the brevity of our route, we required this cyclization to form the seven-membered ring as well as the C6 all-carbon quaternary center. Initially, we planned to use a Conia-ene (see **35**)[33] or Pd-mediated cycloalkylation[34] reaction (see **36**) to accomplish this goal. From **37**, retrosynthetically disconnecting the C3–C4 bond separated the structure into our key functionalized camphor derivative, 8-hydroxycamphor (**5**), and the simple, linear fragment **38**. As our group had previously shown that 5 could be readily accessed from (*S*)-carvone (**1**),[14] the fact that the remainder of the natural product skeleton could be derived from **38** highlighted the appeal of the “camphor first” strategy. In the forward sense, we envisioned converting **38** into a nucleophile that would add to a C8 electrophile formed by oxidation of the alcohol group in **5**. We also anticipated that this coupling would create a functional handle at C3 (see **37** and **34**) that would aid functionalizations of C3 and C5—should they prove difficult using directed C–H functionalization methods. On the basis of this analysis (Figure 3), we commenced our studies on the total synthesis of longiborneol (**8**).

2. Synthesis of Longiborneol.

2.1. Initial Efforts toward Fragment Coupling and Cyclization.—Our synthesis of longiborneol (**8**) began with preparation of the requisite C8-functionalized camphor derivative. Our group has previously reported an enantiospecific synthesis of 8-hydroxycamphor (**5**) from (*S*)-carvone (**1**) using a three-step skeletal remodeling sequence (Figure 4).[14] In this sequence, the isopropenyl moiety of (*S*)-carvone (**1**) was first epoxidized to give **39**, which was then subjected to a Ti(III)-mediated reductive cyclization to give cydobutanols **2** and **3** (see Figure 1A).[35] A modification of the originally reported procedure led to an improved 87% combined yield of a 1.5:1 mixture of diastereomers (52% yield of major diastereomer **2**).[31] Treatment of **2** with a Brønsted acid then effected a semipinacol rearrangement (see **41**) which delivered 8-hydroxycamphor (**5**). Upon reoptimization of this

reaction, we found that the use of *p*-toluenesulfonic acid led to an improved yield of 83% (43% overall yield of **5** from **1**) on multigram scale.[31] The potential to quickly convert the hydroxy group of **5** into several electrophilic functionalities, as well as avoiding the use of toxic reagents in its preparation,[27,36] made it an ideal starting point for our synthesis of longiborneol (**8**).

We expected that converting the primary alcohol of **5** to an aldehyde would provide an ideal electrophile for the fragment coupling. Surprisingly, when **5** was subjected to Dess–Martin periodinane[37] or Ley–Griffith oxidation conditions,[38] carboxylic acid **43** was obtained as the sole product in 81% and 24% yields, respectively (entries 1 and 2, Figure 5A). We hypothesized that aldehyde **42** readily forms hydrated acetals (**45**) with the ketone group in the presence of trace amounts of water (Figure 5B). These acetals then undergo oxidation to the corresponding carboxylic acid (**43**). Attempts to utilize **43** as an alternative electrophile were unsuccessful (see the Supporting Information, p S2). We found that standard TEMPO–PIDA oxidation[39] conditions gave only a trace amount of **42** (entry 3, Figure 5A), but that the addition of more TEMPO and PIDA afforded the product in quantitative yield (entry 4). On the basis of these results and those shown in entries 1 and 2, we postulated that 8-hydroxycamphor (**5**) might exist as a five-membered cyclic acetal under the conditions shown in entry 3, preventing the desired oxidation. However, under the conditions shown in entry 4, we hypothesized that the *in situ* generation of AcOH caused equilibration between the acetal isomers and the keto-alcohol, with the latter undergoing the desired oxidation. Accordingly, we found that the addition of AcOH to the reaction mixture afforded aldehyde **42** in quantitative yield (entry 5). These conditions reproducibly provide **42** on multigram scale, and their discovery set the stage for the exploration of several fragment-coupling reactions.

Treatment of aldehyde **42** with the alkyl lithium reagent prepared from bromide **42** afforded chemoselectively coupled products **47** and **48** (Figure 6A). As the C8 ketone was required for our proposed cyclizations, we attempted to open acetal **48** and protect the resulting alcohol under basic conditions (see **48** → **49**). However, under all the conditions that were investigated for *O*-functionalization (e.g., silylation, alkylation, and acylation), we only observed acetal derived products. For example, when we treated the mixture of **47** and **48** with TBSOTf and 2,6-lutidine, we obtained TBS-acetal **50** as a 1:1 mixture of diastereomers. These results may reflect relatively greater thermodynamic stability of the acetals compared to the open forms of these molecules, which is supported by gas phase calculations for **47** and **48** (B3LYP/6-31G* level of theory, Figure 6B). To circumvent this undesired side reactivity, we next planned to subject the coupled product mixture to oxidation to force the opening of the acetal group in **48**.

Following chemoselective nucleophilic addition into aldehyde **42**, the corresponding crude mixture of **47** and **48** was subjected to DMP-oxidation conditions[37] to provide diketone **51** (Figure 6C). To forge the seven-membered ring from **51**, we attempted a Conia-ene reaction[33] mediated by π-acids, Brønsted/Lewis acids, or thermal conditions. Unfortunately, we observed only complex mixtures without any evidence of desired product **52**. We reasoned that protection of the C3 ketone (see **53**) might enable a Conia-ene reaction,[33]

or that conversion of the C8 ketone to an enol-ether (see **54**) could be followed by a Pd-mediated cycloalkylation.[34] Unfortunately, attempts to synthesize such intermediates led only to enol acetal derivatives. For instance, treatment with TBSOTf and Et_3N gave acetal **55**. These results suggested that the oxygen atom at the C-3 position easily engages the C8 ketone group on the [2.2.1]bicyde, leading to unproductive side reactions.

2.2. Camphor Cyclobutanol Syntheses.—We next sought to protect the ketone group of ketoaldehyde **42** prior to nucleophilic addition to the aldehyde group (see **56**, Figure 7A). However, treating **42** with soft-enolization conditions led to an intramolecular aldol reaction which gave cyclobutanol **57** as a single diastereomer. We envisioned using **57** for fragment coupling reactions as outlined in Figure 7B. However, this approach was unsuccessful, probably due to competing β-scission of the more substituted C–C bond. Alternatively, we found that treating **42** with SmI_2 (Figure 7A)[40] afforded cyclobutanediol **58**, but we were also unable to effect C–C cleavage/fragment coupling cascades with this substrate.

2.3. Olefination Fragment Coupling and Subsequent Attempted Cyclizations.—The results described above suggested that C-3 oxygen-bearing compounds would lead to undesired reactivity. Therefore, we sought to accomplish the fragment coupling using olefrnation chemistry in order to circumvent this problem (Figure 8A). To our delight, treating ketoaldehyde **42** with the ylide prepared from phosphonium bromide **61** afforded diene **62** as a 7:1 Z/E mixture.[41] Anticipating that the isomeric skipped diene might be a more apt substrate for cyclization to form the desired seven-membered ring, we also sought to prepare **64**. Our attempts to synthesize requisite phosphonium bromide **63** were initially complicated by competing isomerization of the terminal alkene group, leading instead to phosphonium bromide **61**. However, by lowering the reaction temperature, we were able to effectively access **63**, and the reaction of the corresponding ylide with ketoaldehyde **42** yielded skipped diene **64** as a single isomer.

With the desired olefination products in hand, we investigated the seven-membered ring formation. Exposing both silyl enol ether **65**[42] and vinyl allyl carbonate **66**[43] to Pd-enolate generation conditions failed to provide any observable cyclization products (Figure 8B). Similarly, attempts to effect a gold-catalyzed Conia-ene reaction returned only starting material.[44] Faced with mounting evidence that closing the tricyclic skeleton of longiborneol (**8**) using these reaction conditions would be extremely challenging, we pivoted to investigating radical cyclizations.

2.4. Radical Cyclization Approach and Synthesis of Copaborneol.—Our initial plan to implement a radical cyclization was to generate a radical at the α-carbon of the ketone group in **62** or **64**. Depending on the diene isomer that was employed, we anticipated a variety of possible cyclization outcomes (Figure 9A). From diene **62**, a seven-endo ring closure would form the desired longibornane core, whereas a six-exo ring closure would give the copabornane core. While the copabornane core would not have been productive for synthesizing longiborneol, it would set the stage for the preparation of the closely related natural product copaborneol (**70**). Similarly, from skipped diene **64**, a seven-exo ring

closure would result in the longibornane core, while an eight-endo cyclization would give a dead-end tricycle (Figure 9A, bottom left). Products corresponding to all of these cyclization possibilities have been observed in related systems,[45] which made it difficult to predict the likely outcome.

To test this plan, we treated diene **62** with KHMDS followed by l,3-dibromo-5,5-dimethylhydantoin (DBDMH) to access bromide **67** as a 7:1 Z/E mixture (Figure 9B). Subjecting **67** to Bu_3SnH and azobis(isobutyronitrile) (AIBN) delivered tricycle **68** and its diastereomer as the sole products through a six-exo-trig radical cyclization. Hydrogenation of the alkene group in **68** and a subsequent dissolving metal reduction of resulting ketone **69** completed a total synthesis of copaborneol (**70**)[32] in 9 steps and 5% overall yield from (*S*)-carvone. We were also able to synthesize the known sesquiterpenoid ylangobomeol from *epi*-**68** (see the Supporting Information, pp S27–S28).

This result signaled that a similar sequence from skipped diene **64** might deliver the longibornane core (Figure 10A). To this end, we prepared bromide **71** from **64**. Unfortunately, we found that treatment of **71** with AIBN and Bu_3SnH led only to nonspecific decomposition.

2.5. Development of an MHAT-Initiated Radical Cyclization.—At this stage, we turned our attention to the use of a metal-hydride hydrogen atom transfer (MHAT) reaction of an enol derivative of **64** (see **72**) as an alternative way to implement a radical cyclization (Figure 10B).[46,47] Under MHAT reaction conditions, we anticipated that tertiary radical **73** would be selectively generated by HAT to the exomethylene group of **72**. This radical would then engage the enol double bond on the [2.2.1]bicycle. The resulting radical at C8 (see **74**) would then either undergo β-scission to afford ketone **75** or proceed through a second HAT to give a reduced ether product.[48] We hypothesized that such a reaction would govern the site selectivity of the cyclization with respect to the side-chain of the molecule, and that the MHAT approach would mitigate concerns related to the steric effects of forming a quaternary center β to the carbonyl given the early transition states associated with radical processes. We also found this MHAT reaction conceptually appealing because it would, in theory, construct the C6–C7 bond while also setting the geminal dimethyl groups of the C6 quaternary center. Using an enol derivative (see **72**) as a radical acceptor would constitute a polarity reversal compared to standard enolate alkylations. We recognized the exciting opportunity this afforded to expand the scope of MHAT methods to polarity-reversed enol alkylation.

The addition of the nucleophilic tertiary radical into an enol acceptor represents a polarity mismatch because enols are electron-rich olefins. This donor–acceptor pair would, therefore, not effectively stabilize a polarized transition state, potentially making radical addition kinetically unfavorable. For example, electrophilic C-centered radicals are often used in reductive or redox-neutral radical couplings to enol derivatives because they lead to a stabilized, polarity-matched transition state (Figure 10C).[49–52] Although there are a few examples employing a wide range of nucleophilic radicals for such couplings, their scope is limited to benzylic or α-ketoester derived enol acceptors (Figure 10D and E).[53,54] We rationalized that the intramolecular nature of our proposed cyclization and use of electron-

poor enol derivatives could mitigate these challenges. We therefore prepared a variety of enol derivatives from **64** to test our hypothesis.

With several enol derivatives in hand (see the Supporting Information, p S3), we began to survey their reactivity under Fe-mediated MHAT conditions (Figure 11).[55,56] When we used silyl enol ether **72a**, a complex mixture was obtained likely because of unproductive competing HAT reactions involving the silyl enol ether.[56] Using vinyl phosphate ester **72b**, which we hoped would readily undergo β-scission to release a stabilized phosphite radical after the initial cyclization,[57] only nonspecific decomposition was observed. Vinyl esters and carbonates were tested next. We hypothesized that, in the case of a vinyl Piv or Boc group, β-scission of the O–C bond would occur from the α-oxy radical, followed by decarbonylation or decarboxylation to generate the stabilized *tert*-butyl radical. When **72c** and **72d** were used, we observed formation of the desired C6–C7 bond. However, the resulting α-oxy radical also underwent a subsequent 5-exo-trig addition to the residual C3–C4 double bond to yield **76** or **77**.

The fact that an additional, undesired, C–C bond was formed when either **72c** or **72d** was used in the MHAT reaction led us to explore other enol derivatives with weaker heteroatom–oxygen bonds. In view of the precedent illustrated in Figure 10E,[54] we turned our attention to vinyl sulfonates. We prepared nonaflate **72e** and subjected it to the screening conditions. Instead of the desired products, we observed fluoroalkyl adduct **78** in 51% yield as a single diastereomer. This product presumably arises through a radical chain process that is initiated when the desired cyclization liberates a sulfonyl radical, which then undergoes desulfonation to give a perfluoroalkyl radical. Addition of this radical to the exomethylene group yields a tertiary radical, which then adds into the vinyl sulfonate—ultimately releasing another sulfonyl radical and propagating the chain. Related trifluoromethylations of vinyl triflates have been reported.[58] We predicted that undesired reactivity of this type would be suppressed if we used a sulfonyl group that was less likely to undergo desulfonylation. To our delight, treatment of vinyl tosylate **72f** with the screening conditions gave rise to the desired cyclized product (**75**) in 60% yield. This reaction constructed the carboskeleton of longiborneol (**8**) and set the stage for the completion of the natural product synthesis.

Tosylate **72f** was difficult to prepare (see the Supporting Information, p S4), but vinyl phenyl sulfonate **72g** proved equally effective in the cyclization (Figure 12). Exposing **72g** to the optimized conditions, which included critical buffering reagents to prevent acid-mediated decomposition (see the Supporting Information, p S6),[56] provided tricycle **75** in 85% yield on multigram scale. Hydrogenation of the residual alkene group afforded longicamphor (**14**), and diastereoselective dissolving-metal-mediated reduction of the carbonyl group of **14** finally furnished longiborneol (**8**). Our synthesis of **8** proceeded in 9 steps from (*S*)-carvone and afforded a remarkable 30% overall yield. Each step of the route is robust and scalable, enabling us to prepare over a gram of **8** in a single pass.

3. Selective Oxygenation of the Longiborneol Scaffold.

Upon completing the total synthesis of longiborneol (**8**), we turned our attention to the selective functionalizations of the longibornane skeleton that would provide access to

oxygenated congeners **23**–**32** (Figure 3).[3–7] Cyclization product **75** was selected as the common intermediate for these divergent syntheses. It featured a C8 hydroxy group, which we envisioned could direct C–H functionalizations at C12 and C15, as well as an alkene group which activated the distal C3 and C5 positions within the seven-membered ring toward oxidation.

3.1. Classic Oxidation Chemistry: Syntheses of 3-Hydroxylongiborneol and 5-Hydroxylongiborneol.—

We began our oxygenation studies by targeting 3-hydroxylongiborneol (**27**) and 5-hydroxylongiborneol (**28**). For the synthesis of **28**, we expected that the C3–C4 alkene group of **75** would activate C5 toward a classic selenium dioxide mediated allylic oxidation (Figure 13A, left). Indeed, treatment with stochiometric selenium dioxide at 80 °C converted olefin **75** to **79** (Figure 13B). Allyhc alcohol **79** was advanced to the natural product by hydrogenation of the alkene group followed by dissolving metal reduction of the ketone group. This route yielded 5-hydroxylongiborneol in 10 total steps and 15% overall yield from (*S*)-carvone.

We hypothesized that Mukaiyama hydration[59] of the alkene group in **75** would lead to an equally straightforward synthesis of 3-hydroxylongiborneol (**27**, Figure 13A, right). Classic Mukaiyama hydration conditions, using THF as a solvent, resulted in sluggish reactivity and incomplete conversion to alcohol **80**—despite multiple additions of $Co(acac)_2$ and phenylsilane. However, using trifluoroethanol as a solvent led to full conversion in 4 h and a dean reaction profile (Figure 13B, see the Supporting Information, p S7 for full details). Fluorinated alcoholic solvents have previously been shown to increase the yields and decrease reaction times of MHAT reactions,[60,61] although their role remains somewhat mysterious. These positive effects may arise because these solvents facilitate the formation of dimeric metal complexes[61,62] or, in the specific case of the Mukaiyama hydration, because they increase the solubility of oxygen in the reaction mixture.[63,64] Alcohol **80** was unstable on silica gel, making it difficult to purify. However, the crude mixture could be directly treated with dissolving metal conditions to afford 3-hydroxylongiborneol in high yield. In total, this route afforded **27** in nine total steps and 26% overall yield from (*S*)-carvone.

3.2. Undirected C–H Oxidation: Syntheses of Culmorone, Culmorin, and 5-Hydroxyculmorin.—

We next investigated the application of undirected C–H oxidation to the functionalization of the longiborneol scaffold. Undirected oxidations of C–H bonds with dioxirane reagents or transition metal catalysts (e.g., the White–Chen catalyst[65]) proceed by hydrogen atom abstraction and capture of the resulting radical, and they tend to selectively oxidize electron-rich and sterically accessible C–H bonds. One tertiary C–H bond in the longiborneol scaffold is α to an inductively withdrawing functional group, and the other is located at the bridgehead position, which would yield a relatively unstable radical. Therefore, we hypothesized that undirected C–H oxidation of a longiborneol derivative would selectively oxidize the methylene positions of the scaffold (Figure 14A). Specifically, we expected the major product to result from oxidation at C4, the most sterically accessible methylene. While C4 oxidation does not correspond to any of the targeted natural products, we also predicted that significant oxygenation at C11 would be observed, as this position

is the only other non-neopentyl methylene and abstraction of a H atom attached to C11 might relieve strain between the pseudoaxial C11 hydrogen atom and the other pseudoaxial groups on the [2.2.1]bicycle. Strain release has been shown to enhance the rate of H atom abstraction in undirected C–H oxidations.[66] Furthermore, oxidation at one position tends to disfavor additional oxygenation at other sites due to the introduction of an additional electron-withdrawing group. As such, we expected each product to be oxidized only at a single site, and we predicted that undirected C–H oxidations could be used to furnish C11 oxidized products which would serve as precursors to culmorone (**26**) and culmorin (**32**).

We selected acetyl longiborneol (**81**, Figure 14B) as the starting material for our undirected C–H oxidation studies. Acetylating the hydroxy group effectively installed an inductively electron-withdrawing group, which we expected to deactivate C8 and C7 toward oxidation (*vide supra*).[65] We began bv treating **81** with the White–Chen catalyst (Fe-(PDP))[65] under a variety of conditions (Figure 14B). Portionwise addition of (*S,S*)-Fe(PDP) to **81** yielded the expected C4 ketone as the major product in 16% yield and the C11 ketone as a minor product in 3% yield. However, the reaction outcome was less selective than hypothesized, as the C3 and C5 ketones were also formed (entry 1). Using (*R,R*)-Fe(PDP) led to similar results, with a slight observed increase in the yield of the C5 oxidized product and a slight decrease in the yield of the C4 oxidized product (entry 2). Slow addition of the catalyst and hydrogen peroxide (entry 3),[67] including at elevated or reduced temperatures (entries 4 and 5), did not lead to observed improvement in the yield of the C11 ketone. Switching the oxidizing reagent to 10 equiv of 3-methyl-(trifluoromethyl)dioxirane (TFDO)[68] led to increased yields of all products (entry 6). Reducing the loading of TFDO further increased product yields (entries 7, 8), but portionwise addition (entry 9)[1] and altering temperature (entry 10) were found to be deleterious. Despite the persistently low yields of the C11 ketone (**83**), the brevity and high overall yield of our longiborneol (**8**) synthesis enabled us to use this reaction to access synthetically useful amounts of **83**.

At scale, treatment of acetyl longiborneol (**81**) with 3 equiv of TFDO yielded an inseparable mixture of C11 ketone **83** and C5 ketone **82** (Figure 14C). Deprotection of the hydroxy groups enabled separation of the components, giving culmorone (**26**) in 2% overall yield over the two steps. Diastereoselective, dissolving metal reduction of the C11 carbonyl in culmorone provided culmorin (**32**) in 12 total steps from (*S*)-carvone and 1% overall yield.

Elucidation of the product mixture resulting from undirected oxidation of acetyl longiborneol (**81**) suggested that we could utilize TFDO-mediated C–H oxidation in a higher yielding synthesis of more oxidized longiborneol congeners. Specifically, we hypothesized that installing an electron-withdrawing group at C5 would deactivate the C3 and C4 positions toward oxidation by TFDO (Figure 15A).[68] Of the sites of oxidation observed on **81**, this would leave only C11 available for functionalization. The resulting C5, C11 bis-functionalized product would map onto 5-hydroxyculmorin (**23**). Therefore, we developed a synthetic route where 5-hydroxylongiborneol (**28**), a natural product which we had previously synthesized (*vide supra*, Figure 13), was bis-acetylated to give **84** (Figure 15B). In accordance with our hypothesis, treatment of **84** with TFDO yielded C11 ketone **85** as the only identifiable product, validating our initial hypothesis. Exposing the crude mixture to dissolving metal conditions effected concomitant reduction of the C11 ketone and global

cleavage of the acetyl groups to give 5-hydroxyculmorin in 13 total steps and 5% overall yield from (*S*)-carvone.

Since our initial disclosure of portions of this work,[31] we have tested other undirected C–H oxidation methods on the longiborneol scaffold. This enabled us to compare the reactivity profiles of these methods to the White–Chen catalyst and TFDO. First, we examined a ruthenium catalyzed C–H oxidation protocol recently published by Griffin et al. (Figure 16A).[69] The authors disclosed two catalysts (Figure 16A, center) which, in conjunction with either an acetic acid or dichloroacetic acid additive (DCAA), are competent for undirected C–H oxidation. After screening each combination of catalyst and additive (Figure 16A, left) we found that the combination of precatalyst **86** and DCAA led to increased yields of the C4 ketone and culmorin precursor **83**, compared to the TFDO mediated reaction (entry 1 vs entry 5). The oxidation to **83** could be carried out on relatively large scale and led to an improved isolated yield of culmorone (Figure 16B). The ruthenium-catalyzed oxidation was also tested for the conversion of **84** to **85** (Figure 16A, right)—the key functionalization in our route to 5-hydroxyculmorin (**23**). Reactions under standard conditions were found to consistently lead to low conversion of **84**, resulting in low yields of **85** (entries 1–4). However, significantly increasing the reaction time also increased conversion and provided **85** in yields comparable to those obtained with TFDO (entry 5).

We next investigated the White–Gormisky–Zhao Catalyst (Mn(CF_3–PDP)) catalysts developed by White and co-workers (Figure 16C).[70–72] Compared to the original White–Chen catalyst, analogues bearing the CF_3-PDP ligand have been found to favor oxidation at less sterically hindered C–H bonds.[72] Additionally, changing the iron-based catalyst to a manganese complex lowers the redox potential and increases the basicity of the metal-oxo intermediate, improving chemoselectivity and, potentially, promoting C–H abstraction.[70,71] To our surprise, we found that using these catalysts under standard conditions led to a mixture of bis-oxidized products: **89**, **90**, and **91** (Figure 16C, left, entries 1–2). Products of this type are unusual under these conditions, as the installation of a ketone group or tertiary alcohol usually deactivates the substrate toward further oxidations. Attempts to suppress the formation of these bis-oxygenated products by lowering the reaction temperature and loadings of catalyst and hydrogen peroxide led to complex product mixtures of bis- and mono-oxygenated products (entries 3–6). Nonetheless, we observed that these conditions, combined with a modified procedure in which both catalyst and hydrogen peroxide were added slowly, led to an increased yield of C11 ketone **83** compared with the reaction using TFDO (see Figure 16A, left, entry 5). The manganese-based catalysts were also tested in the oxidation of **84** (Figure 16C, right). In that case, the (*R,R*) catalyst was found to provide **85** in higher yield than in the reactions using TFDO (entry 1).

In general, these varied reaction conditions led to similar results, with the exception of the White–Gormisky–Zhao catalyst which led to bis-oxygenated products. However, each method leads to different degrees of starting material conversion and yield in the two reactions relevant to our syntheses, highlighting the need for a wide survey of methods when undirected C–H oxidations are employed in complex molecule synthesis.

3.3. Directed C–H Oxidation: Syntheses of 12-Hydroxylongiborneol, 14-Hydroxylongiborneol, and 15-Hydroxylongiborneol.—

We identified directed C–H functionalization methods as being particularly well-suited for the functionalization of the primary C12 C–H bond that would be required for a synthesis of 12-hydroxylongiborneol (**31**). Initially, we predicted that the Sanford acetoxylation,[73] where an oxime is installed to direct C–H acetoxylation of a 1,3-methyl group, would be an ideal tactic for the targeted functionalization (Figure 17A). Unfortunately, after testing a variety of conditions to condense a methoxy-amine or hydroxy-amine[74] onto the ketone group of longicamphor (**14**), or its unsaturated analogue **75**, we found that the desired oximes could not be formed on either substrate (Figure 17B). We hypothesize that these oximes are difficult to synthesize because of the extreme steric hindrance around the neopentyl ketone groups, which are also proximal to another quaternary center. This hypothesis is supported by the fact that methoxime **92** is easily synthesized from skipped diene **64**. However, when **92** was subjected to acetoxylation conditions, only nonspecific decomposition was observed. We chose not to pursue the acetoxylation of similar substrates further in order to investigate other approaches more consistent with our goal of late-stage diversification.

Specifically, we next explored the use of a Hartwig silylation to functionalize C12.[75] To set the stage for this functionalization, in general, a (hydrido)silyl ether is installed on a hydroxy group. Then, an iridium-catalyzed, intramolecular C–H functionalization of a methyl group forges a Si–C bond to give a silacycle. This intermediate is finally converted to a diol product using a Tamao–Fleming oxidation.[76] Initially, we sought to utilize longiborneol (**8**) as a starting material for this reaction sequence. While functionalization of the 1,3-methyl group should have been kinetically favored, it has been shown that conformational effects can lead to different site selectivity.[77] Therefore, we expected that either the C12 or C15 position, which we observed to be proximal to the hydroxy group in the crystal structure of 5-hydroxylongiborneol (**28**), would be functionalized in the directed silylation (Figure 17A). Unfortunately, despite screening several (hydrido)silyl ethers (Figure 17C),[77] we were unable to obtain these products. Instead, we either recovered longiborneol (**8**) as the only identifiable product or observed no reaction in the C–H functionalization-oxidation sequence.

We used a borneol model system to gain insight into this reaction sequence (Figure 17D). Hartwig and co-workers have shown that using isoborneol (**93**) as a starting material leads to diol **94**, in which the bridgehead methyl group is functionalized.[75] Conversely, we found that using bomeol (**95**), which features a pseudoaxial hydroxy group analogous to that found in longiborneol (**8**), led to diol **96** through 1, 3 functionalization of the methylene position. This outcome suggests that the geometric relationship between the pseudoaxial hydroxy group and the bridgehead methyl group does not favor a directed silylation—as methylene silylations can result from starting materials without methyl groups γ to their hydroxy group.[78] Products corresponding to **96** may not be observed when longiborneol (**8**) is used as a starting material because of conformational changes in the [2.2.1]bicycle induced by the tricyclic scaffold.

The silylation selectivity observed in the borneol model system indicated that we might be able to use the Hartwig silylation to effectively functionalize C12 of longiborneol if we

inverted the orientation of the C8 hydroxy group. Accordingly, we treated longicamphor (**14**) with lithium aluminum hydride to obtain C8-*epi* longiborneol (**97**, Figure 17E). Alcohol **97** was then treated with chlorodimethylsilane to yield (hydrido)silyl ether **98**, which smoothly underwent C–H functionalization to give silacycle **99**. Tamao–Fleming oxidation[76] of **99** gave C8-epi 12-hydroxylongiborneol (**100**) in a remarkable 70% yield over the three-step sequence. A net epimerization of the C8 hydroxy-bearing stereocenter of **100** was accomplished by oxidation to ketoaldehyde **101** followed by dissolving metal reduction of both carbonyl groups. This synthetic route produced 12-hydroxylongiborneol (**31**) in 14 total steps and 6% overall yield from (*S*)-carvone.

With 12-hydroxylongiborneol (**31**) in hand, we returned to the C15 functionalization required to synthesize 15-hydroxylongiborneol (**30**). Attempts to use alternative C–H functionalization reactions directed by C8 functional groups proved unproductive (see the Supporting Information, p S8). Instead, we planned an oxidative relay strategy[79] in which a transient functional group would be installed at C5 and used to direct functionalization at C14 (which would correspond to the natural product 14-hydroxylongiborneol) and/or C15 (Figure 18A, top left). We first attempted this plan by synthesizing a C5 oxime from common intermediate **75**, in a six-step sequence. Unfortunately, we found that exposing methoxime **105** to Sanford acetoxylation conditions yielded mostly bis-functionalized product **106** (Figure 18A). We also synthesized free oxime **107** (through a similar sequence) but again found that bis-acetoxylation occurred under the Sanford conditions (**108**, Figure 18A, bottom right).

Presumably these reactions led to bis-acetoxylated products because the desired monoacetoxylated compounds are competent substrates for a subsequent acetoxylation. Conceptually, we reasoned that if the palladation step could be separated from the oxidation of the resulting palladacycle, the monofunctionalized products would be formed selectively. In principle, this separation of the two steps could be implemented with the stoichiometric palladation chemistry first described by Baldwin (Figure 18B).[80] Indeed, treating oxime **107** with a stoichiometric quantity of Na_2PdCl_4 led to bis-palladium complex **109**. Acetylation of the oximes in **109**, followed by treatment with lead(IV) acetate, effected oxidation of the palladacycles to yield monoacetoxylated **110** as a 2:1 mixture of the diastereomeric C14 and C15 acetoxylated products. Treatment of the mixture with iron and acetic acid effected reductive cleavage of the acetyl oxime to the corresponding imine, which hydrolyzed to the ketone upon workup.[81] Condensation with tosylhydrazine followed by a LAH-mediated Caglioti reaction[82] yielded the natural products, which were separable. This route delivered 14-hydroxylongiborneol (**29**) and 15-hydroxylongiborneol (**30**) in 19 total steps and 7% and 4% overall yield from (*S*)-carvone, respectively.

In an effort to avoid the use of stochiometric quantities of palladium and reduce step count, we returned to the optimization of the Sanford acetoxylation (Table 1). As described above, standard conditions[74] using oxime **107** led to a 20% yield of bis-acetoxylated product 108 (entry 1). We were unable to find examples of similar bis-acetoxylated products in the literature, but reasoned that we could limit their formation by limiting the loading of oxidant in the reaction mixture. We found that using a substoichiometric amount of the PIDA oxidant significantly changed the product distribution to favor the monoacetoxylated

products (entry 2), and that using acetyl-oxime **111** increased the yields of all products (entry 3). Remarkably, changing the cosolvent from acetic anhydride to HFIP and lowering the temperature completely suppressed formation of the bis-acetoxylated product (**108**). Unfortunately, these conditions only delivered the monoacetoxylated products in 25% combined yield (entry 4), and we were unable to optimize further (see the Supporting Information, p S9). However, using acetic anhydride as a cosolvent and running the reaction at a lower temperature provided the monoacetoxylated products in 33% combined yield in a 6.6:1 ratio to the bis-acetoxylated product (entry 5). Upon scale-up, **110** was obtained in 41% yield. These reaction conditions both reduced the loading of palladium required for the acetoxylation and shortened the synthesis route to 14-hydroxylongiborneol (**29**) and 15-hydroxylongiborneol (**30**) to 17 total steps from (*S*)-carvone.

3.4. Synthesis of Longifolene.—Our investigations into the late-stage functionalization of the longiborneol core also led to a total synthesis of longifolene (**112**). While attempting the installation of an *N*-methyl-sulfamate ester onto the hydroxy group of longiborneol (**8**)—for a proposed directed C–H bromination at C12[83]—we obtained (−)-longifolene (**112**) as the sole product in high yield (Figure 19A). This constitutes a total synthesis of **112** in 10 steps and 26% overall yield from (*S*)-carvone. A similar rearrangement of the longiborneol core was previously reported by Kuo and Money.[27] However, their strategy relied on converting 8-*epi*-longiborneol (*ent*-**97**) to the corresponding mesylate, resulting in an E2 elimination and concomitant rearrangement to (+)-**112** (Figure 19B). In our case, the rearrangement presumably occurs through an E1 elimination of the *N*-methyl-sulfamate. Interestingly, longifolene (**112**) was used by Corey and co-workers to showcase their concept of strategic bond analysis,[84] with which we juxtapose our “camphor first” strategy (*vide supra*). Notably, our synthesis of longifolene is the shortest reported to date.

4. Expansion of Carvone Remodeling Tactics to Additional Camphor Derivatives.

Having completed syntheses of many longiborneol sesquiterpenoids, we sought to broaden the scope of the carvone to camphor skeletal remodeling approach in order to facilitate future natural product syntheses. We have focused on increasing the diversity of functionalized camphor derivatives that can be accessed from carvone and employed as starting materials. In previous work (Figure 20A), we had shown that C8-, C9-, and C6-functionalized camphor derivatives are readily accessed by skeletal remodeling. That work demonstrated the synthesis of 8-hydroxycamphor (**5**) described above. It also showed that treatment of major diastereomer **2** with *m*-CPBA gave rise to 6,8-dihydroxycamphor (**115**) through a semipinacol rearrangement. Subjecting minor cyclobutanol diastereomer **3** to analogous conditions was also shown to yield 9-hydroxycamphor (**116**) or 6,9-dihydroxycamphor (**117**).

We envisioned that selective allylic oxidation of cyclobutanols **2** and/or **3** would provide an opportunity to access camphor derivatives with functionalization at different sites (Figure 20B). We found that SeO_2 mediated oxidation of the allylic methyl group of protected alcohol **118** afforded diol **119**. Epoxidation of **119** followed by treatment with PPTS (to effect a semipinacol rearrangement) gave camphor triol **120**. Alternatively, we anticipated

that allylic oxidation conditions known to occur through radical intermediates would favor oxidation at the C5 methylene.[85] Due to instability of the cyclobutanol under the required reaction conditions, protected diol **121** was employed in the planned C–H methylene oxidation. We found that treatment of **121** with Collins' reagent in the presence of 4 Å molecular sieves gave enone **122**.[85] Treating **122** with TsOH led to simultaneous cleavage of the acetal protecting group and semipinacol rearrangement. Protection of the resulting primary alcohol group as a TBDPS ether afforded 8-hydroxybornanedione **123**. In this way, camphor derivatives which bear functionality at every unactivated, nonquaternary position of the camphor framework were prepared by scaffold-remodeling of carvone. These compounds should be serviceable intermediates en route to other complex natural products. For example, **120** and **123** map onto the natural products guanacastepene K (**10**)[86] and culmorone (**26**), respectively.

CONCLUSIONS

In this work, we demonstrate a "camphor first" strategy toward the longiborneol sesquiterpenoids, which consisted of distinct skeletal remodeling and C–H functionalization phases. Efficient syntheses of several natural products (in all cases the shortest to date) were realized using this nonconventional synthesis strategy. Fragment coupling by olefination and a subsequent radical-mediated cyclization, to forge the characteristic seven-membered ring, proved to be effective for building the longiborneol scaffold around 8-hydroxycamphor (**5**). Initial investigations of reductive radical cyclizations led to six-membered ring formation and a total synthesis of copaborneol (**70**). Subsequently, we found that an MHAT-derived tertiary radical could engage a vinyl phenyl sulfonate enol radical acceptor (**72g**) to give desired cyclization product **75**. This tricycle was advanced to longibomeol (**8**), completing a nine-step synthesis which demonstrated the merits of our "camphor first" strategy.

The goal of the second phase of this project was to investigate whether C–H functionalization chemistry could be used to access congeners **23**–**32** through late-stage diversification of tricycle **75**. Derivatization of the alkene group in **75** led to syntheses of 3-hydroxylongiborneol (**27**) and 5-hydroxylongiborneol (**28**). Undirected C–H oxidation chemistry was successfully employed to access culmorone (**26**) and culmorin (**32**). Efforts to use a directed Hartwig silylation to functionalize C12 of longiborneol initially proved challenging because of an unfavorable geometric relationship between the C8 hydroxy group and the C12 methyl group. This difficulty was circumvented by inverting the stereochemical configuration of the hydroxy group, enabling access to 12-hydroxylongiborneol (**31**). Use of similar tactics to functionalize C15 proved unsuccessful. Instead, we developed a relay oxidation strategy which provided access to both 14-hydroxylongiborneol (**29**) and 15-hydroxylongiborneol (**30**).

Overall, our work demonstrates the utility of skeletal remodeling tactics in "camphor first" synthesis strategies. Furthermore, it highlights the power of modern C–H functionalization methods to selectively diversify C–H-rich architectures. While challenges associated with installation of directing groups, substrate control, and a lack of selectivity point to improvements that are still necessary for wide adoption of the C–H functionalization methods applied here, they nonetheless enabled functionalization of every natural product-

relevant position of the longiborneol scaffold. Finally, we showed that the carvone-to-camphor skeletal remodeling paradigm can be expanded to novel derivatives. These derivatives are promising starting points for future natural product syntheses.

Supplementary Material

Refer to Web version on PubMed Central for supplementary material.

ACKNOWLEDGMENTS

We are grateful to the National Institutes of Health (NIGMS MIRA R35 GM130345) for grant support and the Molecular Scaffold Design Collective (Agreement No. HR00111890024) of the Defense Advanced Research Projects Agency for partial support of this work. R.F.L. is grateful for fellowship support from the National Science Foundation Graduate Research Fellowships Program (DGE 1752814). G.S. thanks the Uehara Memorial Foundation for a postdoctoral fellowship. The authors acknowledge Dr. Hasan Celik and UC Berkeley's NMR facility in the College of Chemistry (CoC-NMR) for spectroscopic assistance. Instruments in the CoC-NMR are supported in part by NIH S10OD024998. The authors thank Shelby King and Prof. M. Christina White (University of Illinois Urbana–Champaign) for providing White–Gormisky–Zhao catalyst for testing. We are grateful to them and other members of the White group—Chiyoung Ahn and Dr. Jinpeng Zhao—for helpful discussions. The authors thank Dr. Jeremy Griffin, Dr. David Vogt, and Prof. Matthew Sigman (University of Utah) for providing ruthenium precatalysts for testing in the undirected C–H oxidation of our substrates and for helpful discussions. The authors thank N. Settineri (University of California, Berkeley) for single-crystal X-ray diffraction studies.

REFERENCES

(1). Chen K; Baran PS Total synthesis of eudesmane terpenes by site-selective C–H oxidations. Nature 2009, 459, 824–828. [PubMed: 19440196]

(2). Xue Y; Dong G Total Synthesis of Penicibilaenes via C–C Activation-Enabled Skeleton Deconstruction and Desaturation Relay-Mediated C–H Functionalization. J. Am. Chem. Soc 2021, 143, 8272–8277. [PubMed: 34038107]

(3). Bahadoor A; Schneiderman D; Gemmill L; Bosnich W; Blackwell B; Melanson JE; McRae G; Harris LJ Hydroxylation of Longiborneol by a Clm2-Encoded CYP450 Monooxygenase to Produce Culmorin in Fusarium graminearum. J. Nat. Prod 2016, 79, 81–88. [PubMed: 26673640]

(4). Ashley JN; Hobbs BC; Raistrick H Studies in the biochemistry of micro-organisms: The crystalline colouring matters of Fusarium culmorum (W. G. Smith) Sacc. and related forms. Biochem. J 1937, 31, 385–397. [PubMed: 16746350]

(5). Kasitu GC; ApSimon JW; Blackwell BA; Fielder DA; Greenhalgh R; Miller JD Isolation and characterization of culmorin derivatives produced by Fusariumculmorum CMI 14764. Can. J. Chem 1992, 70, 1308–1316.

(6). Alam M; Jones EBG; Hossain MB; van der Helm D Isolation and Structure of Isoculmorin from the Marine Fungus Kallichroma tethys. J. Nat. Prod 1996, 59, 454–456. [PubMed: 8699191]

(7). Barton DHR; Werstiuk H; Sesquiterpenoids N Sesquiterpenoids. Part XIV. The constitution and stereochemistry of culmorin. Journal of the Chemical Society C: Organic 1968, 0, 148–155.

(8). BRIGGS LH; SUTHERLAND MD THE ESSENTIAL OIL OF CUPRESSUS MACROCARPA. J. Org. Chem 1942, 07, 397–407.

(9). Akiyoshi S; Erdtman H; Kubota T Chemistry of the natural order cupressales–XXVI: The identity of junipene, kuromatsuene and longifolene and of juniperol, kuromatsuol, macrocarpol and longiborneol. Tetrahedron 1960, 9, 237–239.

(10). Brill ZG; Condakes ML; Ting CP; Maimone TJ Navigating the Chiral Pool in the Total Synthesis of Complex Terpene Natural Products. Chem. Rev 2017, 117, 11753–11795. [PubMed: 28293944]

(11). Lusi RF; Perea MA; Sarpong R C–C. Bond Cleavage of α-Pinene Derivatives Prepared from Carvone as a General Strategy for Complex Molecule Synthesis. Acc. Chem. Res 2022, 55, 746–758. [PubMed: 35170951]

(12). (a)Kuroda Y; et al. Isolation, synthesis and bioactivity studies of phomactin terpenoids. Nat. Chem 2018, 10, 938–945. [PubMed: 30061613] (b)Leger PR; Kuroda Y; Chang S; Jurczyk J; Sarpong R C–C. Bond Cleavage Approach to Complex Terpenoids: Development of a Unified Total Synthesis of the Phomactins. J. Am. Chem. Soc 2020, 142, 15536–15547. [PubMed: 32799452]

(13). (a)Norseeda K; Gasser V; Sarpong R A Late-Stage Functionalization Approach to Derivatives of the Pyrano[3,2-a]carbazole Natural Products. J. Org. Chem 2019, 84, 5965–5973. [PubMed: 30969773] (b)Haley HMS; Payer SE; Papidocha SM; Clemens S; Nyenhuis J; Sarpong R Bioinspired Diversification Approach Toward the Total Synthesis of Lycodine-Type Alkaloids. J. Am. Chem. Soc 2021, 143, 4732–4740. [PubMed: 33729783]

(14). Masarwa A; Weber M; Sarpong R Selective C–C and C–H Bond Activation/Cleavage of Pinene Derivatives: Synthesis of Enantiopure Cyclohexenone Scaffolds and Mechanistic Insights. J. Am. Chem. Soc 2015, 137, 6327–6334. [PubMed: 25892479]

(15). Weber M, Owens K; Masarwa A; Sarpong R Construction of Enantiopure Taxoid and Natural Product-like Scaffolds Using a C–C Bond Cleavage/Arylation Reaction. Org. Lett 2015, 17, 5432–5435. [PubMed: 26485318]

(16). Kerschgens I; Rovira AR; Sarpong R Total Synthesis of (−)-Xishacorene B from (R)-Carvone Using a C–C Activation Strategy. J. Am. Chem. Soc 2018, 140, 9810–9813. [PubMed: 30032603]

(17). Money T Camphor: a chiral starting material in natural product synthesis. Nat. Prod. Rep 1985, 2, 253. [PubMed: 3906448]

(18). (a)Kitamura M; Chiba S; Narasaka K Synthesis of (±)-Sordaricin. Chem. Lett 2004, 33, 942–943. (b)Chiba S; Kitamura M; Narasaka K Synthesis of (−)-Sordarin. J. Am. Chem. Soc 2006, 128, 6931–6937. [PubMed: 16719473]

(19). (a)Mander LN; Thomson RJ Total Synthesis of Sordaricin. Org. Lett 2003, 5, 1321–1324. [PubMed: 12688749] (b)Mander LN; Thomson RJ; Total Synthesis of Sordaricin. J. Org. Chem 2005, 70, 1654–1670. [PubMed: 15730285]

(20). Kato N; Kusakabe S;Wu X; Kamitamari M; Takeshita H Total synthesis of optically active sordaricin methyl ester and its Λ2-derivative. J. Chem. Soc, Chem. Commun 1993, 0, 1002–1004.

(21). Nicolaou KC; Ortiz A; Zhang H; Dagneau P; Lanver A; Jennings MP; Arseniyadis S; Faraoni R; Iizos DE Total Synthesis and Structural Revision of Vannusals A and B: Synthesis of the Originally Assigned Structure of Vannusal B. J. Am. Chem. Soc 2010, 132, 7138–7152. [PubMed: 20443561]

(22). (a)Ihara M; Makita K; Fujiwara Y; Tokunaga Y; Fukumoto K Stereoselective Construction of Copaborneol and Longiborneol Frameworks by Intramolecular Double Michael Reaction. J. Org. Chem 1996, 61, 6416–6421. [PubMed: 11667485] (b)Takasu K; Mizutani S; Noguchi M; Makita K; Ihara M Total Synthesis of (±)-Culmorin and (±)-Longiborneol: An Efficient Construction of Tricyclo[6.3.0.03,9]undecan-10-one by Intramolecular Double Michael Addition. J. Org. Chem 2000, 65, 4112–4119. [PubMed: 10866628]

(23). (a)Welch SC; Walters RL Total Syntheses of (+)-Longicamphor and (+)-Longiborneol. Synth. Commun 1973, 3, 419–423.(b)Welch SC; Walters RL Stereoselective total syntheses of (+-)-Iongicyclene, (+-)-longicamphor, and (+-)-longiborneol. J. Org. Chem 1974, 39, 2665–2673.

(24). Corey EJ; Howe WJ; Orf HW; Pensak DA; Petersson G General methods of synthetic analysis. Strategic bond disconnections for bridged polycyclic structures. J. Am. Chem. Soc 1975, 97, 6116–6124.

(25). Marth CJ; Gallego GM; Lee JC; Lebold TP; Kulyk S; Kou KGM; Qin J; Lilien R; Sarpong R Network-analysis-guided synthesis of weisaconitine D and liljestrandinine. Nature 2015, 528, 493–498. [PubMed: 26675722]

(26). Hanson JR; Nyfeler R Studies in terpenoid biosynthesis. Part 18. Biosynthesis of culmorin. J. Chem. Soc., Perkin Trans 1 1976, 2471–2475.

(27). (a)Kuo DL; Money T An enantiospecific synthesis of longiborneol and longifolene. J. Chem. Soc, Chem. Commun 1986, 0, 1691–1692.(b)Kuo DL,; Money T Enantiospecific synthesis of longiborneol and longifolene. Can. J. Chem 1988, 66, 1794–1804.

(28). Arndtsen BA; Bergman RG; Mobley TA; Peterson TH Selective Intermolecular Carbon-Hydrogen Bond Activation by Synthetic Metal Complexes in Homogeneous Solution. Acc. Chem. Res 1995, 28, 154–162.

(29). White MC; Zhao J Aliphatic C–H Oxidations for Late-Stage Functionalization. J. Am. Chem. Soc 2018, 140, 13988–14009. [PubMed: 30185033]

(30). Qiu Y; Gao S Trends in applying C–H oxidation to the total synthesis of natural products. Nat. Prod. Rep 2016, 33, 562–581. [PubMed: 26847167]

(31). Lusi RF; Sennari G; Sarpong R Total synthesis of nine longiborneol sesquiterpenoids using a functionalized camphor strategy. Nat. Chem 2022, 14, 450–456. [PubMed: 35165424]

(32). (a)Kolbe M; Westfelt L Copaborneol, the Major Sesquiterpene Alcohol in Pinus silvestris Wood and Sulphate Turpentine. Acta Chem. Scand 1967, 21, 585–587.(b)Bohlmann F; Suding H; Cuatrecasas J; Robinson H; King RM Tricyclic sesquiterpenes and further diterpenes from Espeletiopsis species. Phytochemistry 1980, 19, 2399–2403.

(33). Rouessac F; Beslin P; Conia J-M La cyclisation thermique des cetones cycliques $\epsilon\zeta$-ethyleniques. Voie d'acces aux cetones polycycliques. Tetrahedron Lett. 1965, 6, 3319–3323.

(34). Streuff J; White DE; Virgil SC; Stoltz BM A palladium-catalysed enolate alkylation cascade fbr the formation of adjacent quaternary and tertiary stereocentres. Nature Chem. 2010, 2, 192–196. [PubMed: 20697457]

(35). Bermejo FA; Fernández Mateos A; Marcos Escribano A; Martín Lago R; Mateos Burón L; Rodríguez López M; Rubio González R Ti(III)-promoted cyclizations. Application to the synthesis of (E)-endo-bergamoten-12-oic acids. Moth oviposition stimulants isolated from Lycopersicon hirsutum. Tetrahedron 2006, 62, 8933–8942.

(36). Eck CR; Mills RW; Money T A new regiospecific synthesis of 8-bromocamphor. J. Chem. Soc., Perkin Trans 1 1975, 251–254.

(37). Dess DB; Martin JC Readily accessible 12-I-5 oxidant for the conversion of primary and secondary alcohols to aldehydes and ketones. J. Org. Chem 1983, 48, 4155–4156.

(38). Griffith WP; Ley SV; Whitcombe GP; White AD Preparation and use of tetra-n-butylammonium per-ruthenate (TBAP reagent) and tetra-n-propylammonium per-ruthenate (TPAP reagent) as new catalytic oxidants for alcohols. J. Chem. Soc., Chem. Commun 1987, 1625–1627.

(39). De Mico A; Margarita R; Parlanti L; Vescovi A; Piancatelli G A Versatile and Highly Selective Hypervalent Iodine (III)/2,2,6,6-Tetramethyl-1-piperidinyloxyl-Mediated Oxidation of Alcohols to Carbonyl Compounds. J. Org. Chem 1997, 62, 6974–6977.

(40). Nomura R; Matsuno T; Endo T Samarium Iodide-Catalyzed Pinacol Coupling of Carbonyl Compounds. J. Am. Chem. Soc 1996, 118, 11666–11667.

(41). Wittig G; Schöllkopf U Über Triphenyl-phosphin-methylene als olefinbildende Reagenzien (I. Mitteil. Chem. Ber 1954, 87, 1318–1330.

(42). Nicolaou KC; Tria GS; Edmonds DJ; Kar M Total Syntheses of (±)-Platencin and (−)-Platencin. J. Am. Chem. Soc 2009, 131, 15909–15917. [PubMed: 19824676]

(43). Shimizu I; Minami I; Tsuji J Palladium-catalyzed synthesis of α,β-unsaturated ketones from ketones via allyl enol carbonates. Tetrahedron Lett. 1983, 24, 1797–1800.

(44). Xiao Y-P; Liu X-Y; Che C-M Efficient Gold(I)-Catalyzed Direct Intramolecular Hydroalkylation of Unactivated Alkenes with α-Ketones. Angew. Chem., Int. Ed 2011, 50, 4937–4941.

(45). (a)Sato T; Ishida S; Ishibashi H; Ikeda M Regiochemistry of radical cyclisations (6-exo/7-endo and 7-exo/8-endo) of N-(o-alkenylphenyl)-2,2-dichloroacetamides. J. Chem. Soc., Perkin Trans. 1 1991, 0, 353–359.(b)Liu L; Chen Q; Wu Y-D; Li C 8-Endo versus 7-Exo Cyclization of α-Carbamoyl Radicals. A Combination of Experimental and Theoretical Studies. J. Org. Chem 2005, 70, 1539–1544. [PubMed: 15730271] (c)Long H; Song J; Xu H-C Electrochemical synthesis of 7-membered carbocycles through cascade 5-exo-trig/7-endo-trig radical cyclization. Org. Chem. Front 2018, 5, 3129–3132.

(46). Crossley SWM; Obradors C; Martinez RM Shenvi RA Mn-, Fe-, and Co-Catalyzed Radical Hydrofunctionalizations of Olefins. Chem. Rev 2016, 116, 8912–9000. [PubMed: 27461578]

(47). Wu J; Ma Z Metal-hydride hydrogen atom transfer (MHAT) reactions in natural product synthesis. Organic Chemistry Frontiers 2021, 8, 7050–7076.

(48). Shevick SL; Wilson CV; Kotesova S; Kim D; Holland PL; Shenvi RA Catalytic hydrogen atom transfer to alkenes: a roadmap for metal hydrides and radicals. Chem. Sci 2020, 11, 12401–12422. [PubMed: 33520153]

(49). Next reference contains examples which only utilize electrophilic radicals as coupling partners.

(50). (a)Dang H-S; Elsegood MRJ; Kim K-M; Roberts BP Radical-chain reductive alkylation of electron-rich alkenes mediated by silanes in the presence of thiols as polarity-reversal catalysts. J. Chem. Soc., Perkin Trans 1 1999, 2061–2068.(b)Fava E; Nakajima M; Tabak MB; Rueping M Tin-free visible light photoredox catalysed cyclisation of enamides as a mild procedure for the synthesis of γ-lactams. Green Chem. 2016, 18, 4531–4535.(c)Giese B; Horler H; Leising M Umpolungsreaktionen mit dem Malonyl-Radikal. Chem. Ber 1986, 119, 444–452.(d)Huang Q; Suravarapu SR; Renaud P A Giese reaction for electron-rich alkenes. Chemical Science 2021, 12, 2225–2230.(e)Melchiorre P; Spinnato D; Schweitzer-Chaput B; Goti G; Ošeka M A Photochemical Organocatalytic Strategy for the α-Alkylation of Ketones using Radicals. Angew. Chem., Int. Ed 2020, 59, 9485–9490.(f)Nakajima M; Lefebvre Q; Rueping M Visible light photoredox-catalysed intermolecular radical addition of α-halo amides to olefins. Chem. Commun 2014, 50, 3619–3622.(g)Renaud P; Schubert S Reductive Alkylation of Enamines with Chloromethyl p-Tolyl Sulfone via a Radical Chain Process. Angewandte Chemie International Edition in English 1990, 29, 433–434.(h)Schubert S; Renaud P; Carrupt P-A; Schenk K Stereoselectivity of the Radical Reductive Alkylation of Enamines: Importance of the Allylic 1,3-Strain Model. Helv. Chim. Acta 1993, 76, 2473–2489.(i)Sumino S; Fusano A; Ryu I Reductive Bromine Atom-Transfer Reaction. Org. Lett 2013, 15, 2826–2829. [PubMed: 23697921] (j)Zard SZ The Xanthate Route to Ketones: When the Radical Is Better than the Enolate. Acc. Chem. Res 2018, 51, 1722–1733. [PubMed: 29932322] (k)Hu B; Chen H; Liu Y; Dong W; Ren K; Xie X; Xu H; Zhang Z Visible light-induced intermolecular radical addition: facile access to γ-ketoesters from alkyl-bromocarboxylates and enamines. Chem. Commun 2014, 50, 13547–13550.

(51). Next references contain very limited examples with nucleophilic radicals.

(52). (a)Song H-J; Lim CJ; Lee S; Kim S Tin-free radical alkylation of ketones viaN-silyloxy enamines. Chem. Commun 2006, 2893–2895.(b)Crossley SWM; Barabé F; Shenvi RA Simple, Chemoselective, Catalytic Olefin Isomerization. J. Am. Chem. Soc 2014, 136, 16788–16791. [PubMed: 25398144] (c)Watanabe Y; Yoneda T; Ueno Y; Toru T Radical reaction of acetonyltributylstannane with α-(phenylseleno) carbonyl compounds: a novel procedure for preparation of 1,4-dicarbonyl compounds. Tetrahedron Lett. 1990, 31, 6669–6672.(d)Cai Y; Roberts BP Carbon–carbon bond formation by radical addition–fragmentation reactions of O-tert-alkyl enols and O-cyclopropylcarbinyl enols. Tetrahedron Lett. 2003, 44, 4645–4648.(e)Cai Y; Roberts BP; Tocher DA; Barnett SA Carbon–carbon bond formation by radical addition–fragmentation reactions of O -alkylated enols. Organic & Biomolecular Chemistry 2004, 2, 2517–2529. [PubMed: 15326533]

(53). (a)Fu M-C; Shang R; Zhao B; Wang B; Fu Y Photocatalytic decarboxylative alkylations mediated by triphenylphosphine and sodium iodide. Science 2019, 363, 1429–1434. [PubMed: 30923218] (b)Miura K; Fujisawa N; Saito H; Wang D; Hosomi A Synthetic Utility of Stannyl Fnolates as Radical Alkylating Agents1. Org. Lett 2001, 3, 2591–2594. [PubMed: 11483068]

(54). Lee JY; Lim K-C; Meng X; Kim S Radical Alkylations of Alkyl Halides and Unactivated C-H Bonds Using Vinyl Triflates. Synlett 2010, 2010, 1647–1650.

(55). Lo JC; Yabe Y; Baran PS A Practical and Catalytic Reductive Olefin Coupling. J. Am. Chem. Soc 2014, 136, 1304–1307. [PubMed: 24428607]

(56). Lo JC; Gui J; Yabe Y; Pan C-M; Baran PS Functionalized olefin cross-coupling to construct carbon–carbon bonds. Nature 2014, 516, 343–348. [PubMed: 25519131]

(57). Maddigan-Wyatt J; Hooper JF Phosphorus Compounds as Precursors and Catalysts for Radical C–C Bond-Forming Reactions. Advanced Synthesis & Catalysis 2021, 363, 924–936.

(58). (a)Su X; Huang H; Yuan Y; Li Y Radical Desulfur-Fragmentation and Reconstruction of Enol Triflates: Facile Access to α-Trifluoromethyl Ketones. Angew. Chem., Int. Ed 2017, 56, 1338–1341.(b)Liu S; Jie J; Yu J; Yang X Visible light induced Trifluoromethyl Migration: Easy Access to α-Trifluoromethylated Ketones from Enol Triflates. Advanced Synthesis & Catalysis 2018, 360, 267–271.

(59). Isayama S; Mukaiyama T A New Method for Preparation of Alcohols from Olefins with Molecular Oxygen and Phenylsilane by the Use of Bis(acetylacetonato)cobalt(II). Chem. Lett 1989, 18, 1071–1074.

(60). Pfaffenbach M; Bakanas I; O'Connor NR; Herrick JL; Sarpong R Total Syntheses of Xiamycins A, C, F, H and Oridamycin A and Preliminary Evaluation of their Anti-Fungal Properties. Angew. Chem., Int. Ed 2019, 58, 15304–15308.

(61). Green SA; Huffman TR; McCourt RO; van der Puyl V; Shenvi RA Hydroalkylation of Olefins To Form Quaternary Carbons. J. Am. Chem. Soc 2019, 141, 7709–7714. [PubMed: 31030508]

(62). Lo JC; Kim D; Pan C-M; Edwards JT; Yabe Y; Gui J; Qin T; Gutiérrez S; Giacoboni J; Smith MW; Holland PL; Baran PS Fe-Catalyzed C–C Bond Construction from Olefins via Radicals. J. Am. Chem. Soc 2017, 139, 2484–2503. [PubMed: 28094980]

(63). Battino R; Rettich TR; Tominaga T The Solubility of Oxygen and Ozone in Liquids. J. Phys. Chem. Ref. Data 1983, 12, 163–178.

(64). Sánchez MA; Mainar AM; Pardo JI; López MC; Urieta JS Solubility of nonpolar gases in 2,2,2-trifluoroethanol and 1,1,1,3,3,3-hexafluoropropan-2-ol at several temperatures and 101.33 kPa partial pressure of gas. Can. J. Chem 2001, 79, 1460–1465.

(65). (a)Chen MS; White MC A Predictably Selective Aliphatic C–H Oxidation Reaction for Complex Molecule Synthesis. Science 2007, 318, 783–787. [PubMed: 17975062] (b)Chen MS; White MC Combined Effects on Selectivity in Fe-Catalyzed Methylene Oxidation. Science 2010, 327, 566–571. [PubMed: 20110502]

(66). Zou L; Paton RS; Eschenmoser A; Newhouse TR; Baran PS; Houk KN Enhanced Reactivity in Dioxirane C–H Oxidations via Strain Release: A Computational and Experimental Study. J. Org. Chem 2013, 78, 4037–4048. [PubMed: 23461537]

(67). Vermeulen NA; Chen MS; Christina White M The Fe(PDP)-catalyzed aliphatic C–H oxidation: a slow addition protocol. Tetrahedron 2009, 65, 3078–3084.

(68). Curci R; D'Accolti L; Fusco C A Novel Approach to the Efficient Oxygenation of Hydrocarbons under Mild Conditions. Superior Oxo Transfer Selectivity Using Dioxiranes. Acc. Chem. Res 2006, 39, 1–9. [PubMed: 16411734]

(69). Griffin JD; Vogt DB; Du Bois J; Sigman MS Mechanistic Guidance Leads to Enhanced Site-Selectivity in C–H Oxidation Reactions Catalyzed by Ruthenium bis (Bipyridine) Complexes. ACS Catal. 2021, 11, 10479–10486.

(70). Chambers RK; Zhao J; Delaney CP; White MC Chemoselective Tertiary C–H Hydroxylation for Late-Stage Functionalization with Mn(PDP)/Chloroacetic Acid Catalysis. Advanced Synthesis & Catalysis 2020, 362, 417–423. [PubMed: 32165875]

(71). Zhao J; Nanjo T; de Lucca EC; White MC Chemoselective methylene oxidation in aromatic molecules. Nature Chem. 2019, 11, 213–221. [PubMed: 30559371]

(72). Gormisky PE; White MC Catalyst-Controlled Aliphatic C–H Oxidations with a Predictive Model for Site-Selectivity. J. Am. Chem. Soc 2013, 135, 14052–14055. [PubMed: 24020940]

(73). Desai LV; Hull KL; Sanford MS Palladium-Catalyzed Oxygenation of Unactivated sp3 C–H Bonds. J. Am. Chem. Soc 2004, 126, 9542–9543. [PubMed: 15291549]

(74). Neufeldt SR; Sanford MS O-Acetyl Oximes as Transformable Directing Groups for Pd-Catalyzed C–H Bond Functionalization. Org. Lett 2010, 12, 532–535. [PubMed: 20041702]

(75). Simmons EM; Hartwig JF Catalytic functionalization of unactivated primary C–H bonds directed by an alcohol. Nature 2012, 483, 70–73. [PubMed: 22382981]

(76). (a)Tamao K; Ishida N; Kumada M (Diisopropoxymethylsilyl)methyl Grignard reagent: a new, practically useful nucleophilic hydroxymethylating agent. J. Org. Chem 1983, 48, 2120–2122. (b)Fleming I; Henning R; Plaut H The phenyl-dimethylsilyl group as a masked form of the hydroxy group. J. Chem. Soc., Chem. Commun 1984, 29–31.

(77). Ma X; Kucera R; Goethe OF; Murphy SK; Herzon SB Directed C–H Bond Oxidation of (+)-Pleuromutilin. J. Org. Chem 2018, 83, 6843–6892. [PubMed: 29664634]

(78). Li B; Driess M; Hartwig JF Iridium-Catalyzed Regioselective Silylation of Secondary Alkyl C–H Bonds for the Synthesis of 1,3-Diols. J. Am. Chem. Soc 2014, 136, 6586–6589. [PubMed: 24734777]

(79). (a)Renata H; Zhou Q; Baran PS Strategic Redox Relay Enables A Scalable Synthesis of Ouabagenin, A Bioactive Cardenolide. Science 2013, 339, 59–63. [PubMed: 23288535] (b)Berger M; Knittl-Frank C; Bauer S; Winter G; Maulide N Application of Relay C–H Oxidation Logic to Polyhydroxylated Oleanane Triterpenoids. Chem. 2020, 6, 1183–1189.

(80). Baldwin JE; Jones RH; Najera C; Yus M Functionalisation of unactivated methyl groups through cyclo-palladation reactions. Tetrahedron 1985, 41, 699–711.

(81). Siler DA; Mighion JD; Sorensen EJ An Enantiospecific Synthesis of Jiadifenolide. Angew. Chem., Int. Ed 2014, 53, 5332–5335.

(82). Caglioti L; Magi M The reaction of tosylhydrazones with lithium aluminium hydride. Tetrahedron 1963, 19, 1127–1131.

(83). Sathyamoorthi S; Banerjee S; Du Bois J; Burns NZ; Zare RN Site-selective bromination of sp3 C–H bonds. Chem. Sci 2018, 9, 100–104. [PubMed: 29629078]

(84). Corey EJ; Ohno M; Vatakencherry PA; Mitra RB TOTAL SYNTHESIS OF d,l-LONGIFOLENE. J. Am. Chem. Soc 1961, 83, 1251–1253.

(85). Fullerton DS; Chen C-M In Situ Allylic Oxidations With Collins Reagent. Synth. Commun 1976, 6, 217–220.

(86). Brady SF; Bondi SM; Clardy J The Guanacastepenes: A Highly Diverse Family of Secondary Metabolites Produced by an Endophytic Fungus. J. Am. Chem. Soc 2001, 123, 9900–9901. [PubMed: 11583556]

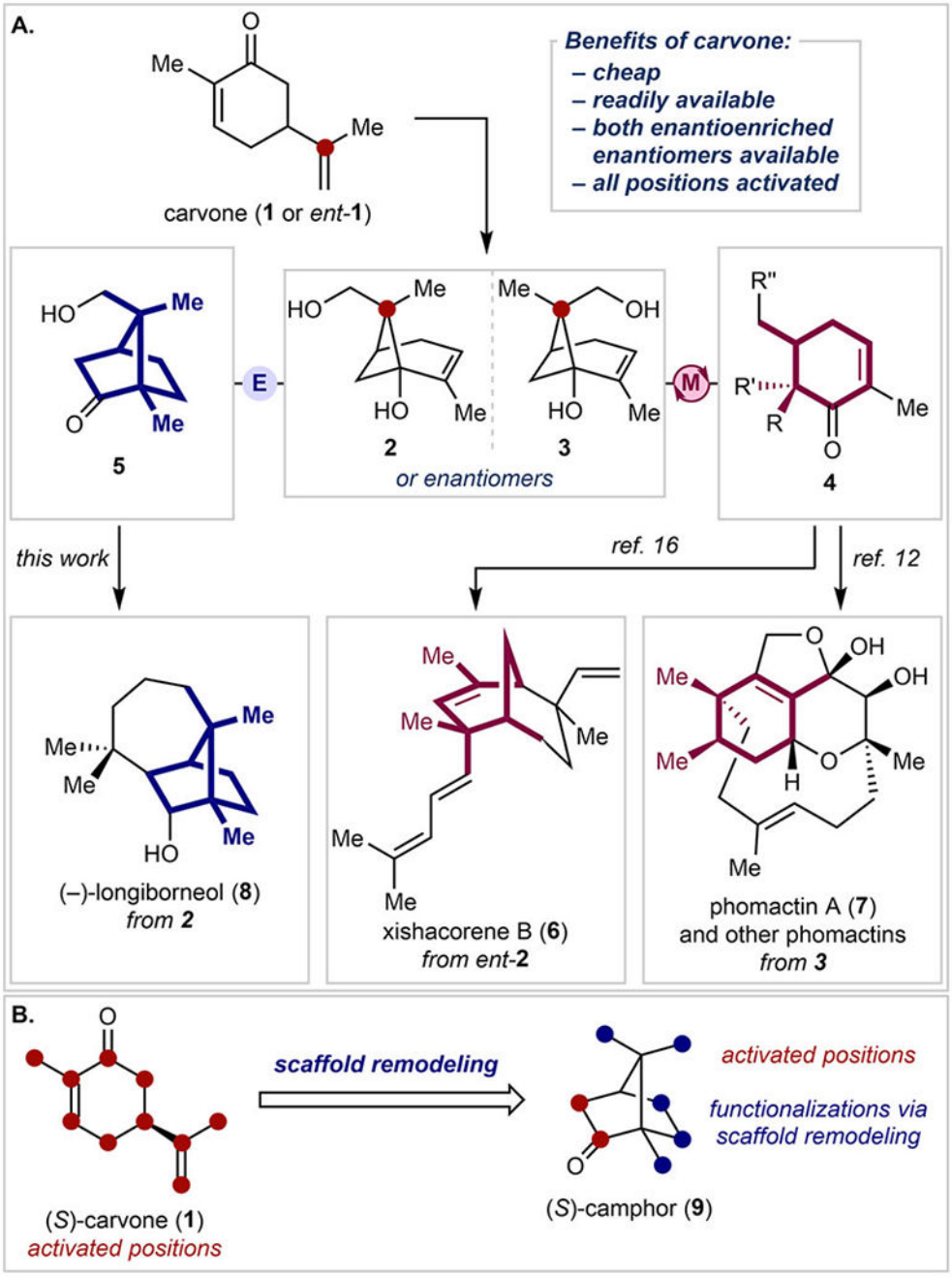

Figure 1.

(A) Skeletal remodeling of carvone and its applications in total synthesis. (B) Skeletal remodeling for the preparation of camphor analogues.

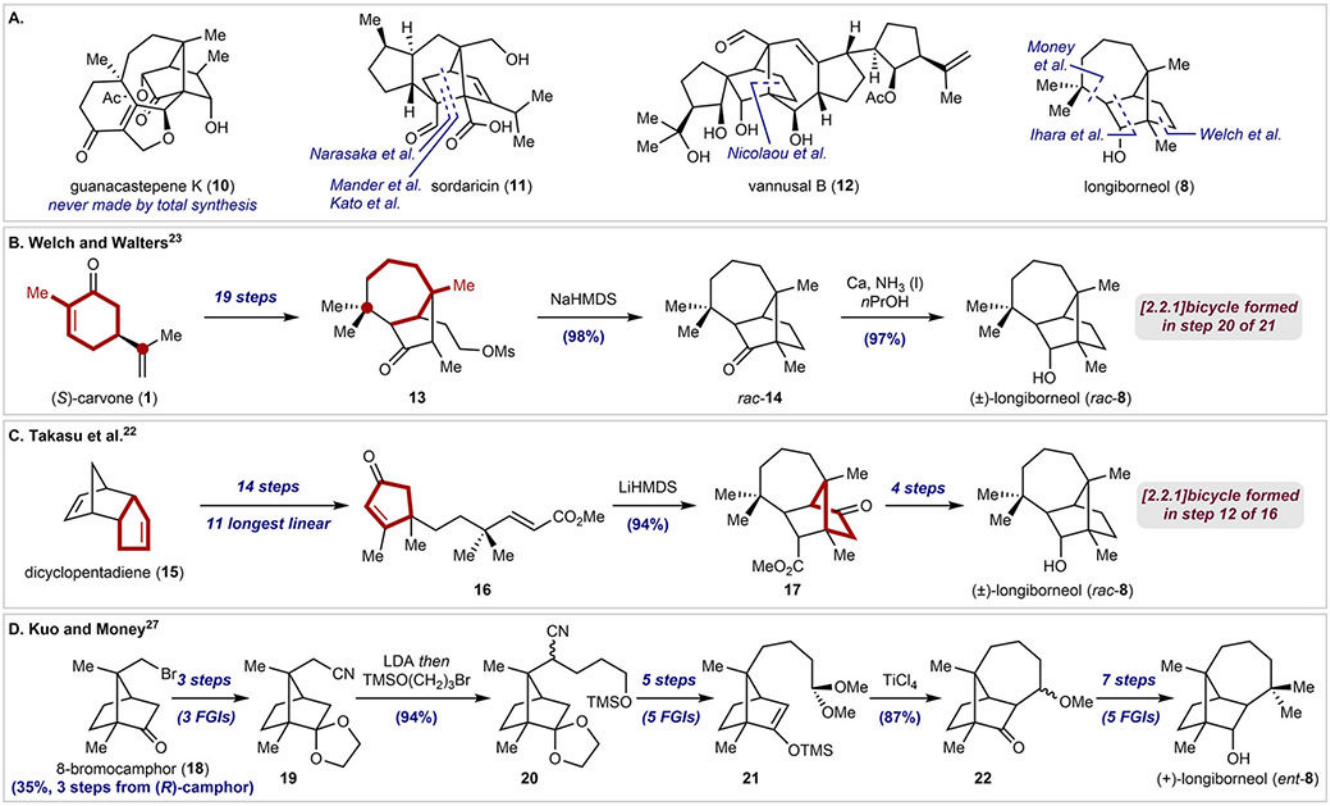

Figure 2.

(A) Selected natural products featuring bornane subskeletons.[18–23] (B) Summary of Welch's total synthesis of longiborneol.[23] (C) Summary of Ihara's total synthesis of longiborneol.[22] (D) Summary of Kou and Money's total synthesis of longiborneol.[27]

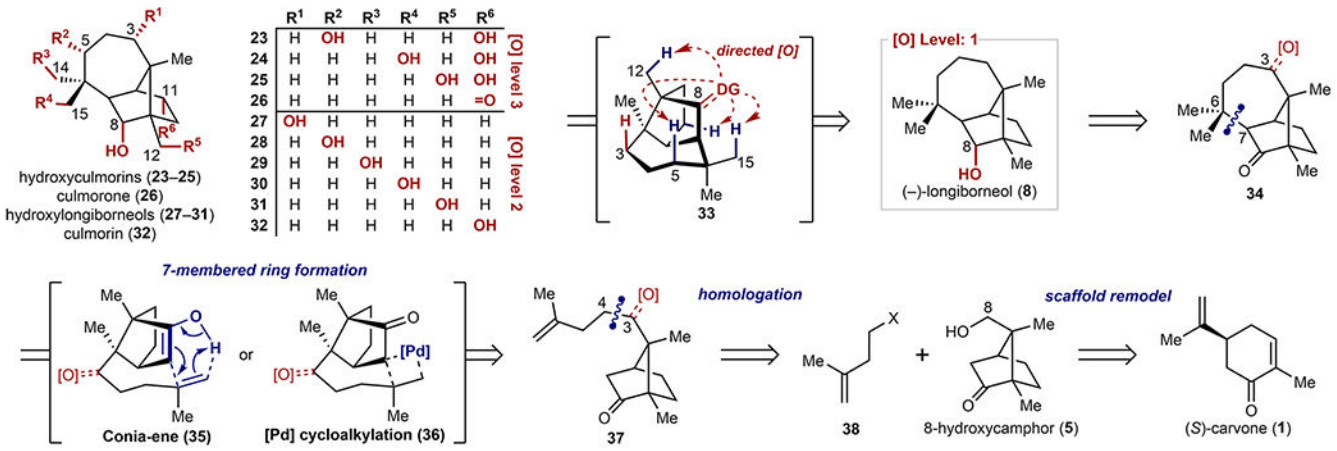

Figure 3.
Our retrosynthesis of longiborneol.

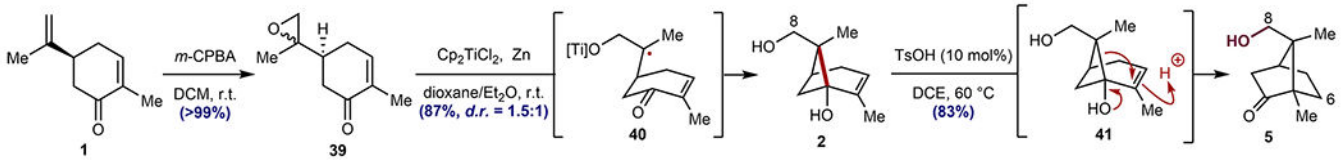

Figure 4.
Synthesis of 8-hydroxycamphor, previously developed by our group.[14]

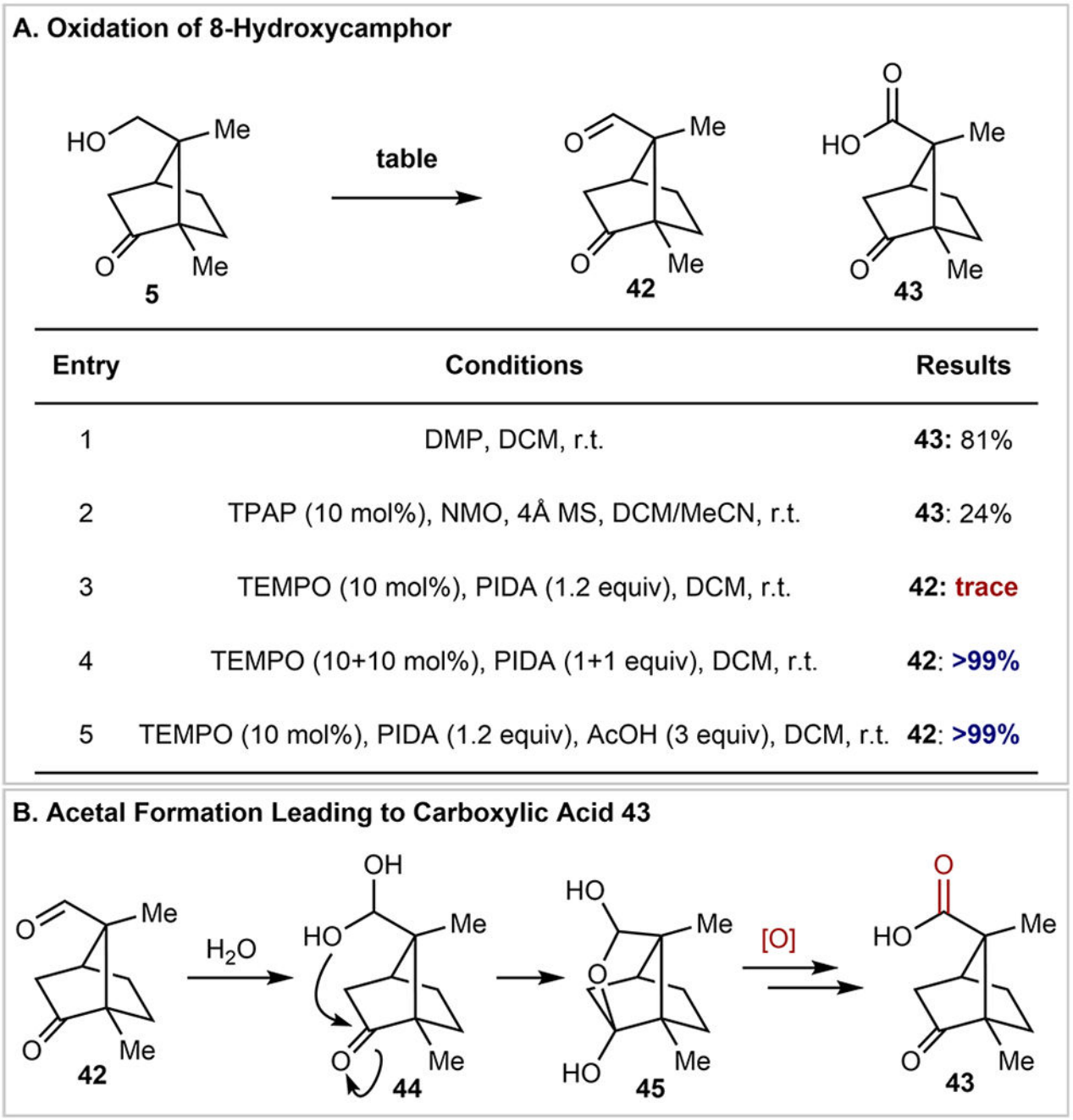

Entry	Conditions	Results
1	DMP, DCM, r.t.	**43:** 81%
2	TPAP (10 mol%), NMO, 4Å MS, DCM/MeCN, r.t.	**43**: 24%
3	TEMPO (10 mol%), PIDA (1.2 equiv), DCM, r.t.	**42: trace**
4	TEMPO (10+10 mol%), PIDA (1+1 equiv), DCM, r.t.	**42**: **>99%**
5	TEMPO (10 mol%), PIDA (1.2 equiv), AcOH (3 equiv), DCM, r.t.	**42**: **>99%**

Figure 5.
(A) 8-Hydroxycamphor oxidation. (B) Proposed mechanism for carboxylic acid formation.

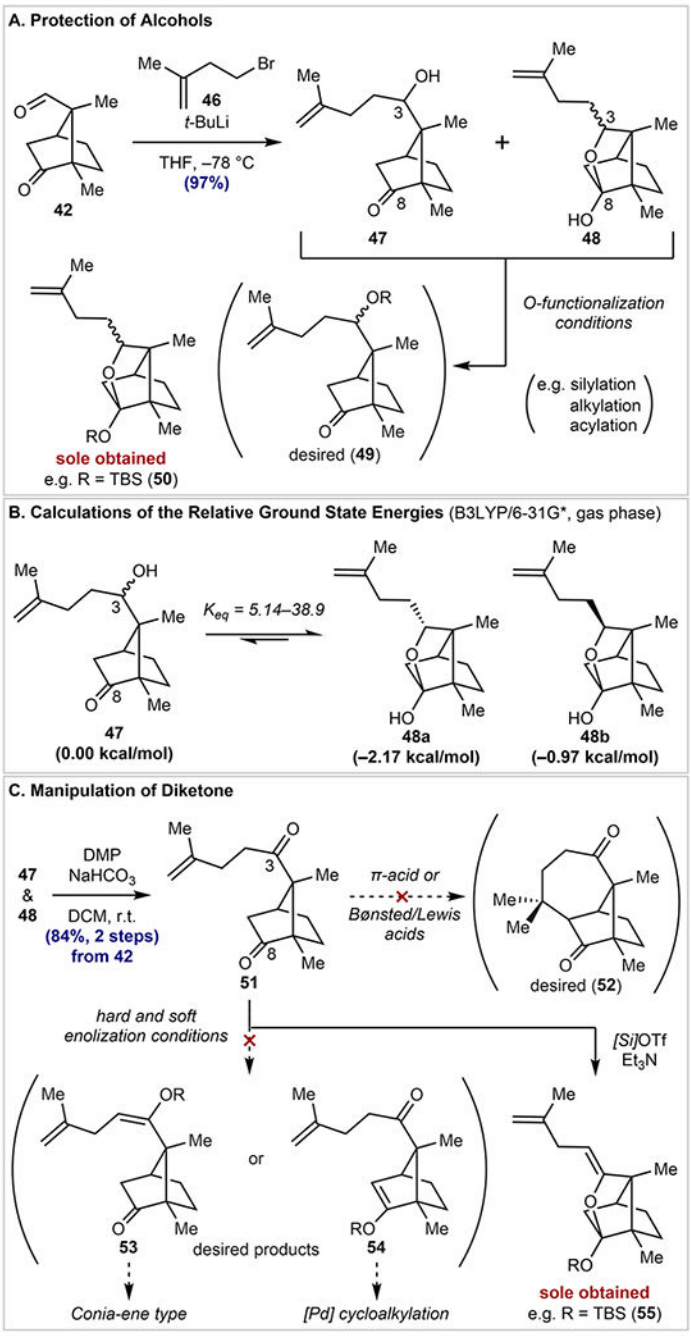

Figure 6.

(A) Addition into aldehyde **42** and subsequent functionalization. (B) Calculated ground-state energies of **47**, **48a**, and **48b**. (C) Oxidation and attempts at seven-membered ring formation.

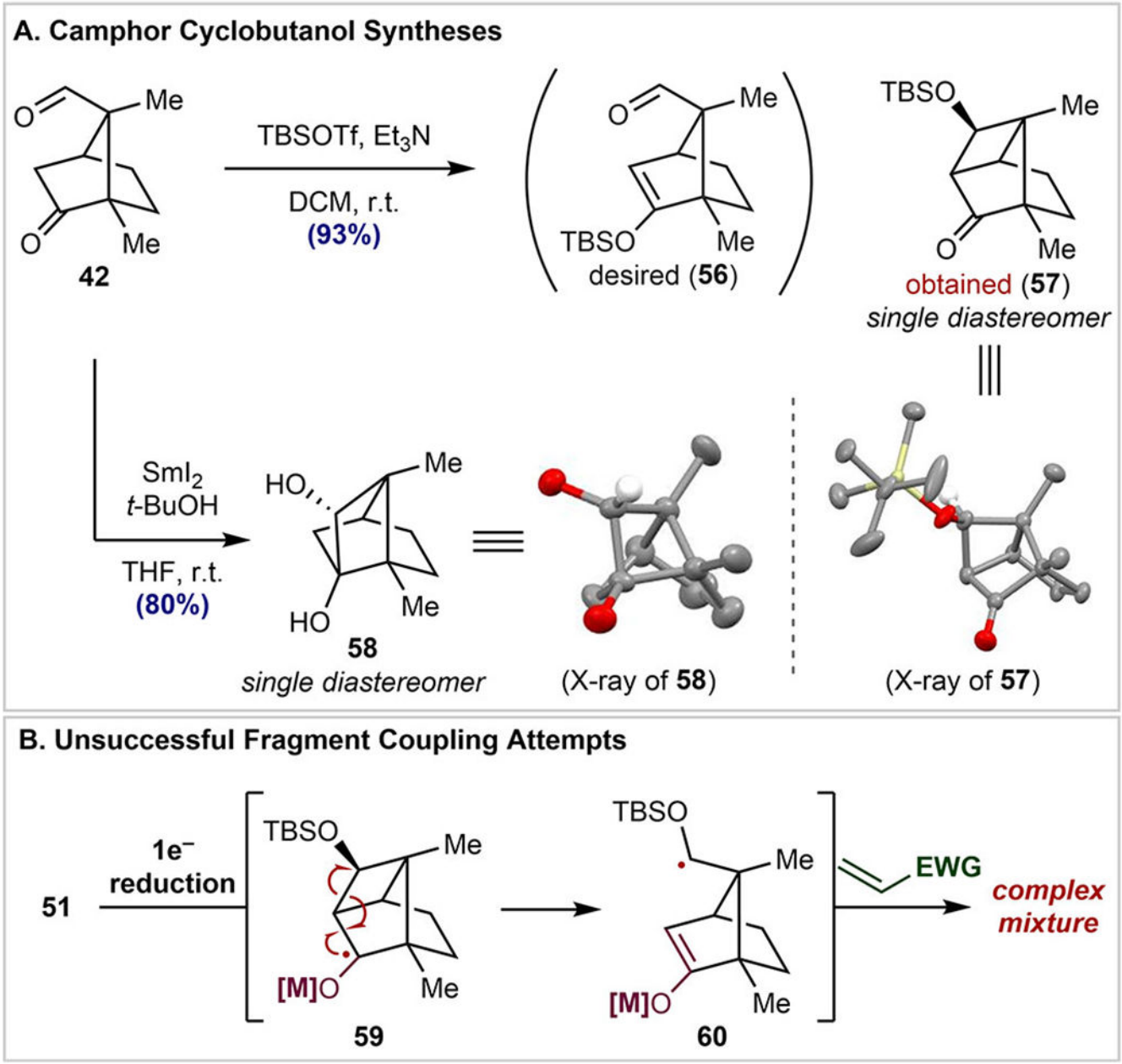

Figure 7.

(A) Synthesis of camphor cyclobutanols **57** and **58**. (B) Proposed one-electron reduction approach to the fragment coupling.

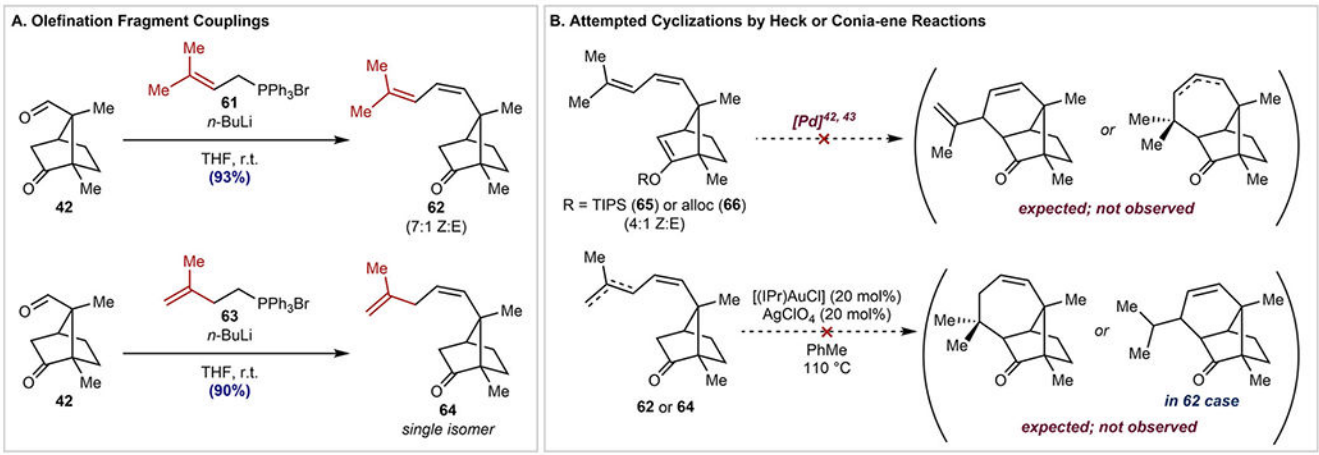

Figure 8.

(A) Olefination fragment couplings. (B) Attempted Pd-mediated cyclizations and Conia-ene[33] reactions to form cyclized products.

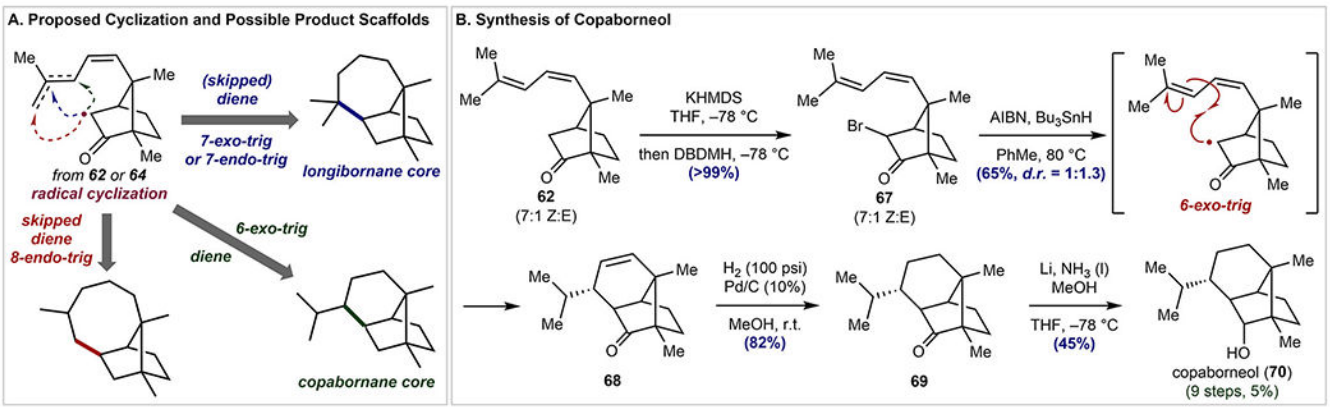

Figure 9.

(A) Potential radical cyclization pathways. (B) Synthesis of copaborneol (**70**)[32] enabled by reductive radical cyclization of bromide **67** to tricycle **68**.

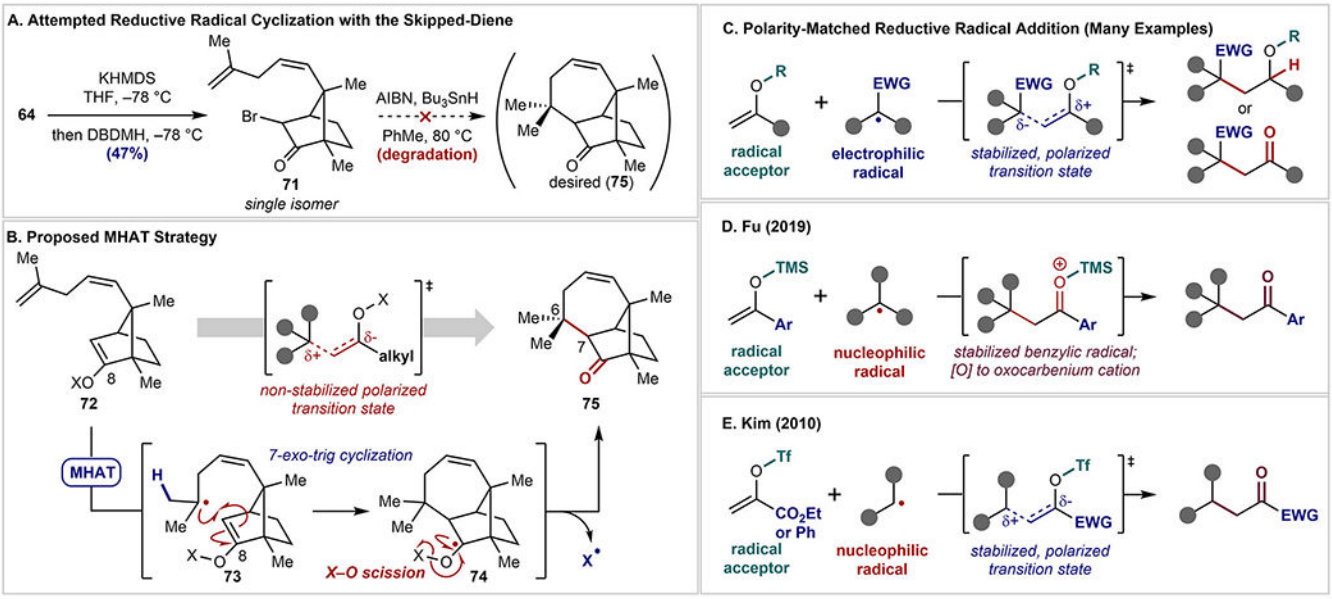

Figure 10.

(A) Attempted reductive radical cyclization with **71**. (B) Proposed MHAT-initiated cyclization. (C) Summary of precedents using polarity matched donor–acceptor pairs.[50] (D and E) Summary of Fu et al. and Kim et al. nucleophilic radical additions into benzylic or α-ketoester-derived acceptors.[53,54]

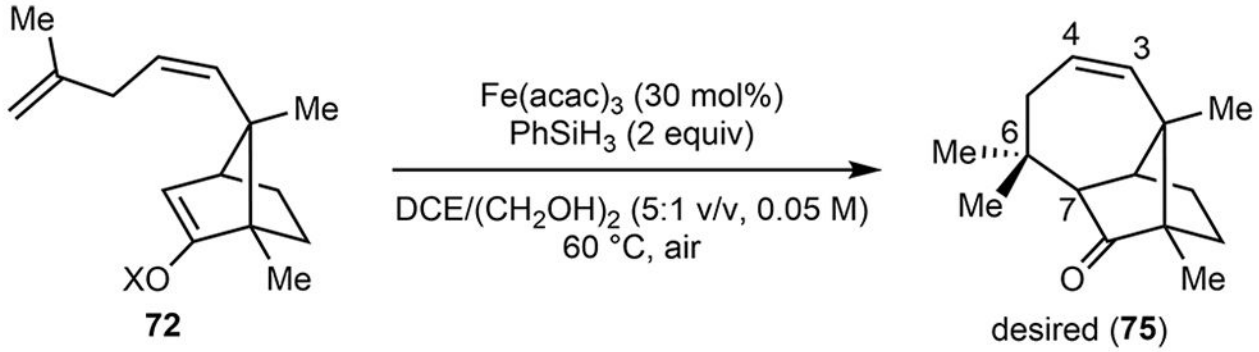

Substrate	Result	Substrate	Result
X = TES (**72a**)	*complex mixture*	X = P(O)(OPh)$_2$ (**72b**)	*decomposition*
X = Piv (**72c**)	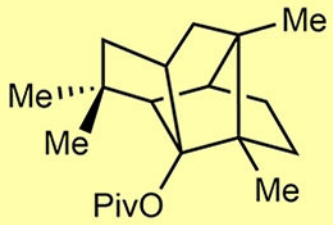 **76: 51%**	X = Boc (**72d**)	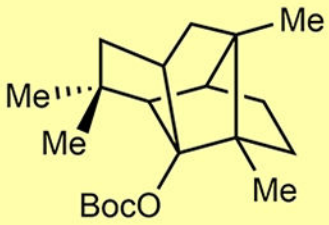 **77: 52%**
X = Nf (**72e**)	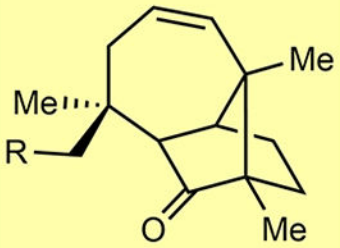 **78: 51%** (R = $(CF_2)_3CF_3$)	X = Ts (**72f**)	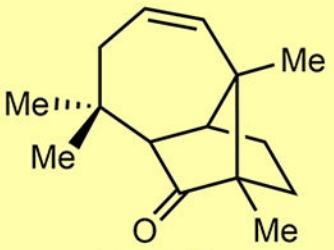 **75: 60%**

Figure 11.
Substrate screening for the MHAT-initiated cyclization.

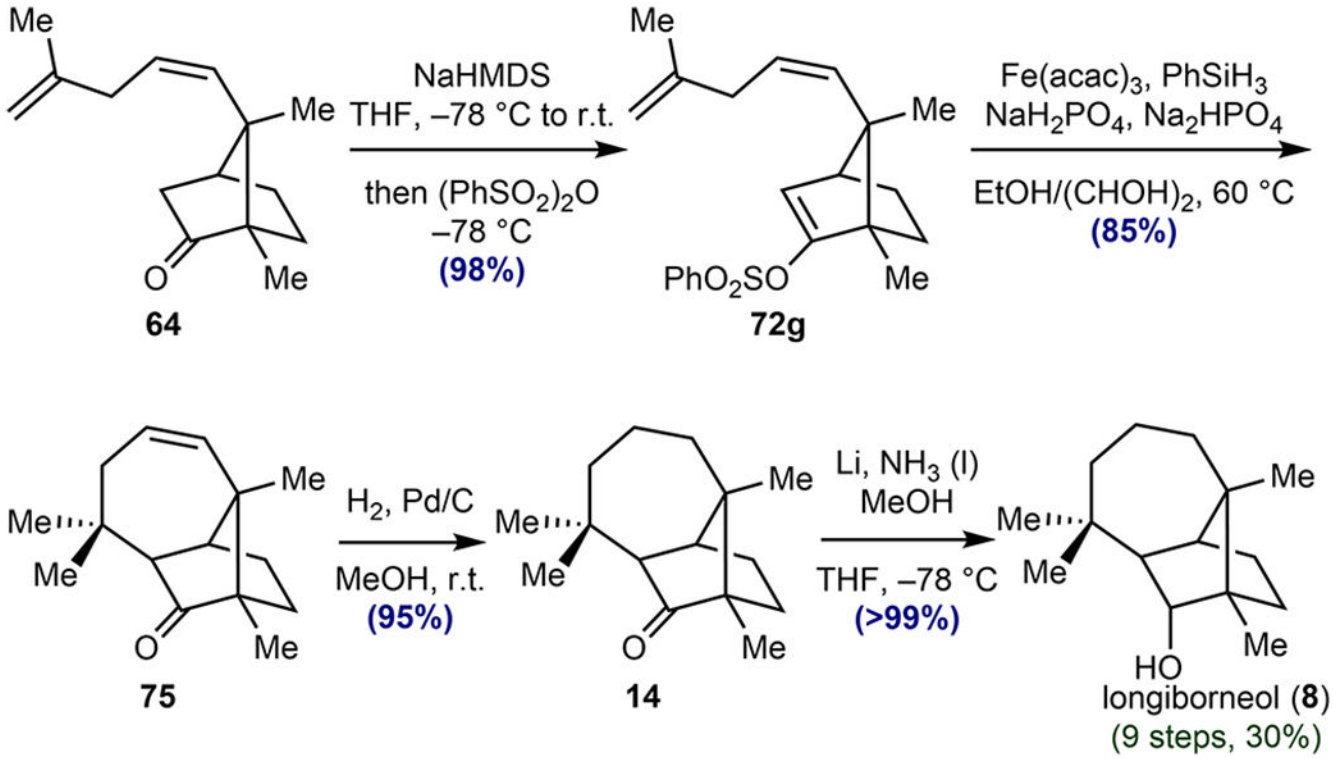

Figure 12.
Completed total synthesis of longiborneol (**8**).

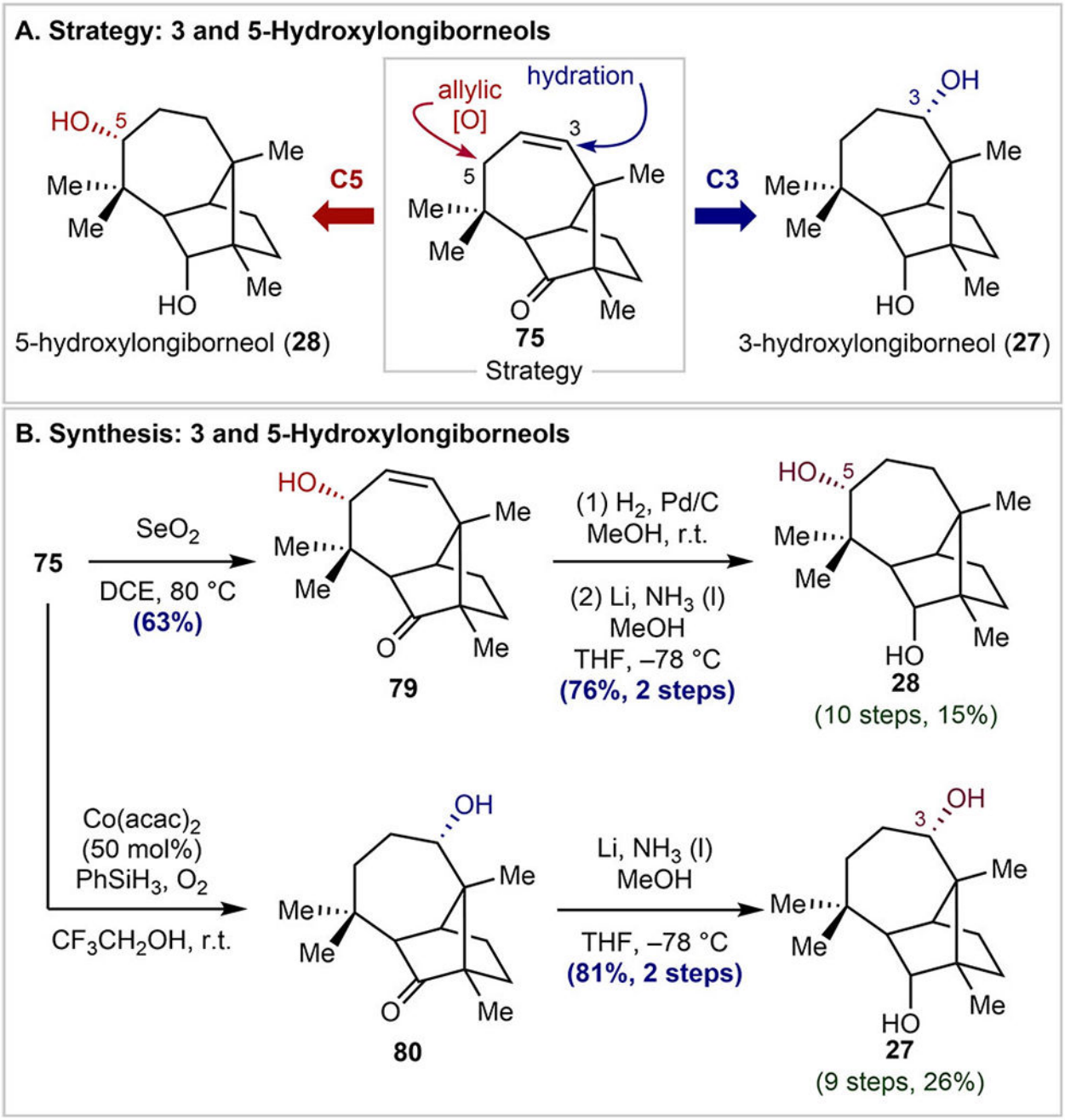

Figure 13.

(A) Oxygenation strategy for preparation of 3- and 5-hydroxylongiborneols. (B) Completed syntheses of 3-hydroxylongiborneol (**27**) and 5-hydroxylongiborneol (**28**).

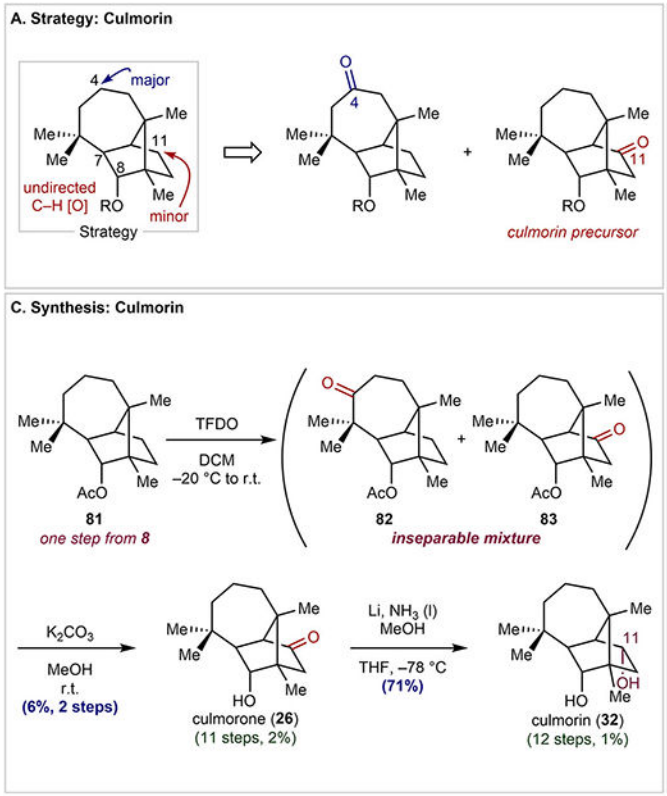

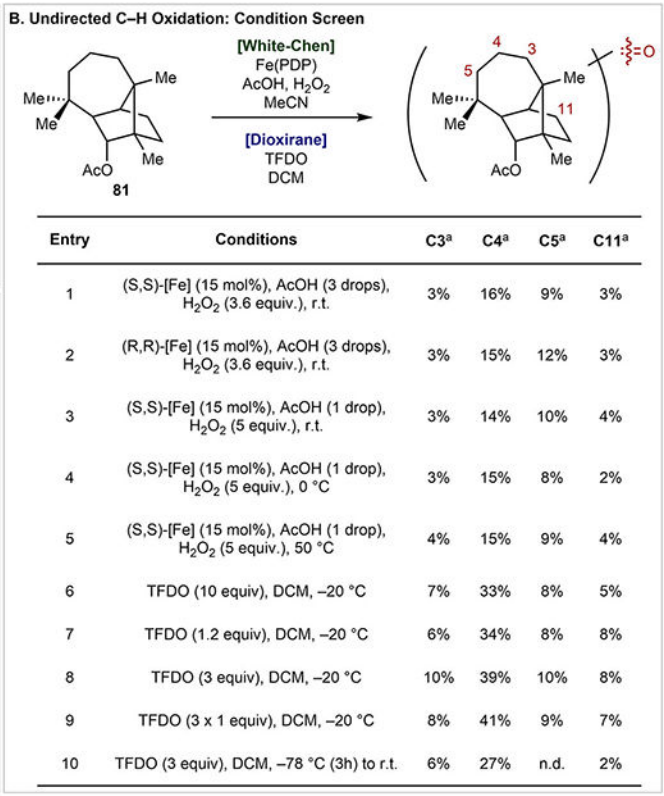

Entry	Conditions	C3[a]	C4[a]	C5[a]	C11[a]
1	(S,S)-[Fe] (15 mol%), AcOH (3 drops), H_2O_2 (3.6 equiv.), r.t.	3%	16%	9%	3%
2	(R,R)-[Fe] (15 mol%), AcOH (3 drops), H_2O_2 (3.6 equiv.), r.t.	3%	15%	12%	3%
3	(S,S)-[Fe] (15 mol%), AcOH (1 drop), H_2O_2 (5 equiv.), r.t.	3%	14%	10%	4%
4	(S,S)-[Fe] (15 mol%), AcOH (1 drop), H_2O_2 (5 equiv.), 0 °C	3%	15%	8%	2%
5	(S,S)-[Fe] (15 mol%), AcOH (1 drop), H_2O_2 (5 equiv.), 50 °C	4%	15%	9%	4%
6	TFDO (10 equiv), DCM, –20 °C	7%	33%	8%	5%
7	TFDO (1.2 equiv), DCM, –20 °C	6%	34%	8%	8%
8	TFDO (3 equiv), DCM, –20 °C	10%	39%	10%	8%
9	TFDO (3 x 1 equiv), DCM, –20 °C	8%	41%	9%	7%
10	TFDO (3 equiv), DCM, –78 °C (3h) to r.t.	6%	27%	n.d.	2%

Figure 14.

(A) Oxygenation strategy for the synthesis of culmorin (**32**). (B) Optimization of the undirected C–H oxidation of acetylated longiborneol (**81**). (C) Complete synthetic routes to culmorone (**26**) and culmorin (**32**). [a] Yields by qNMR.

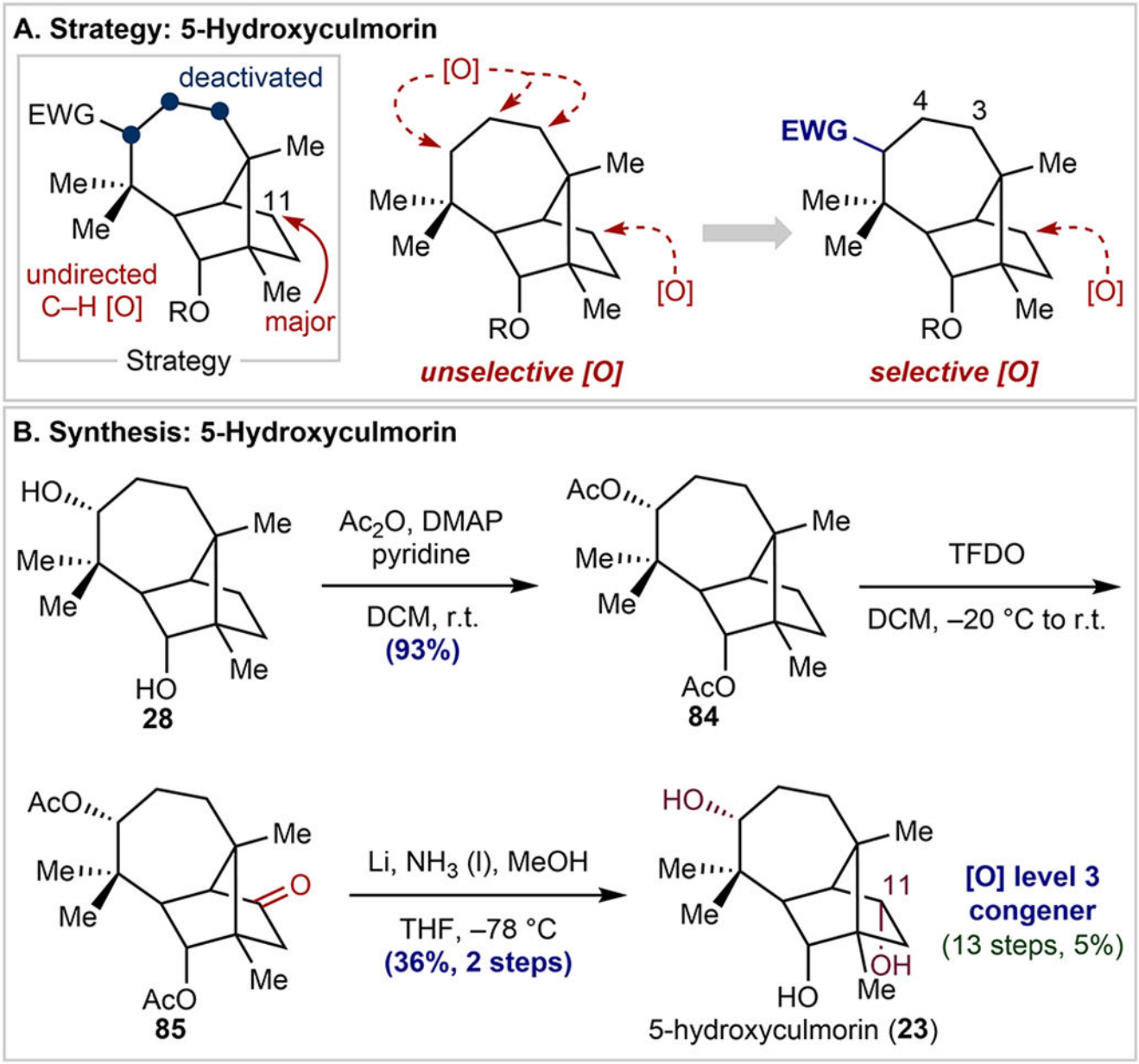

Figure 15.

(A) Oxygenation strategy for our synthesis of 5-hydroxyculmorin (**23**). (B) Synthetic route to 5-hydroxyculmorin (**23**).

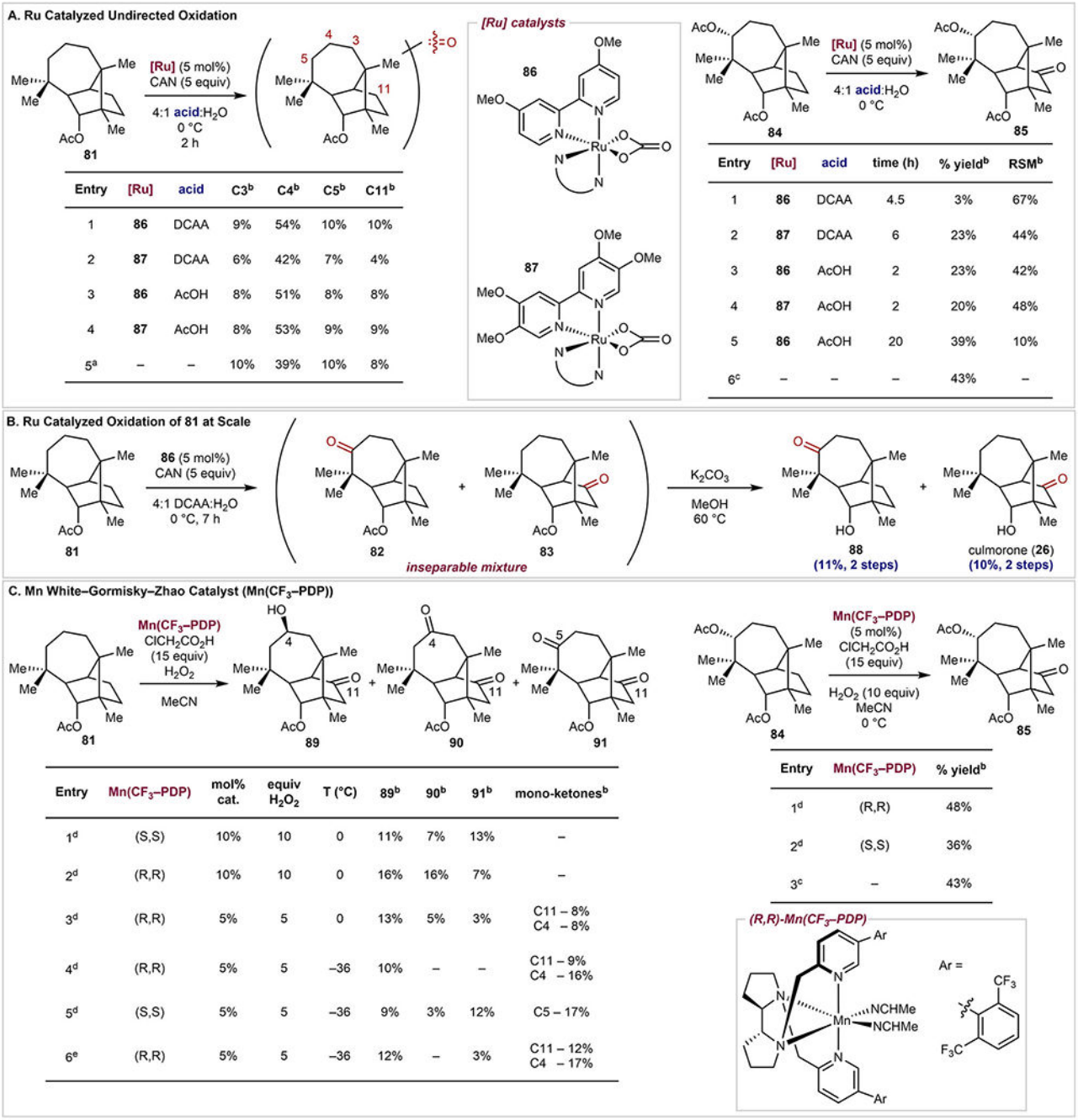

Entry	[Ru]	acid	C3[b]	C4[b]	C5[b]	C11[b]
1	86	DCAA	9%	54%	10%	10%
2	87	DCAA	6%	42%	7%	4%
3	86	AcOH	8%	51%	8%	8%
4	87	AcOH	8%	53%	9%	9%
5[a]	–	–	10%	39%	10%	8%

Entry	[Ru]	acid	time (h)	% yield[b]	RSM[b]
1	86	DCAA	4.5	3%	67%
2	87	DCAA	6	23%	44%
3	86	AcOH	2	23%	42%
4	87	AcOH	2	20%	48%
5	86	AcOH	20	39%	10%
6[c]	–	–	–	43%	–

Entry	Mn(CF3–PDP)	mol% cat.	equiv H_2O_2	T (°C)	89[b]	90[b]	91[b]	mono-ketones[b]
1[d]	(S,S)	10%	10	0	11%	7%	13%	–
2[d]	(R,R)	10%	10	0	16%	16%	7%	–
3[d]	(R,R)	5%	5	0	13%	5%	3%	C11 – 8% C4 – 8%
4[d]	(R,R)	5%	5	–36	10%	–	–	C11 – 9% C4 – 16%
5[d]	(S,S)	5%	5	–36	9%	3%	12%	C5 – 17%
6[e]	(R,R)	5%	5	–36	12%	–	3%	C11 – 12% C4 – 17%

Entry	Mn(CF3–PDP)	% yield[b]
1[d]	(R,R)	48%
2[d]	(S,S)	36%
3[c]	–	43%

Figure 16.

(A) Screening of Ru-mediated undirected C–H oxidation conditions.[69] (B) Application of optimal conditions to the synthesis of culmorone (**26**) upon scale-up. (C) Screening of Mn White–Chen catalyst-mediated C–H oxidation conditions.[70] [a]TFDO (3 equiv), DCM, −20 °C. [b]Yields by qNMR. [c](1) TFDO (3 equiv), DCM (0.032 M), −20 °C; (2) TFDO (9 equiv), DCM (0.032 M) −20 °C–rt. [d]H_2O_2 added over 3 h by syringe pump. [e](*R,R*)-Mn(CF_3-PDP) and H_2O_2 added over 3 h by syringe pump.

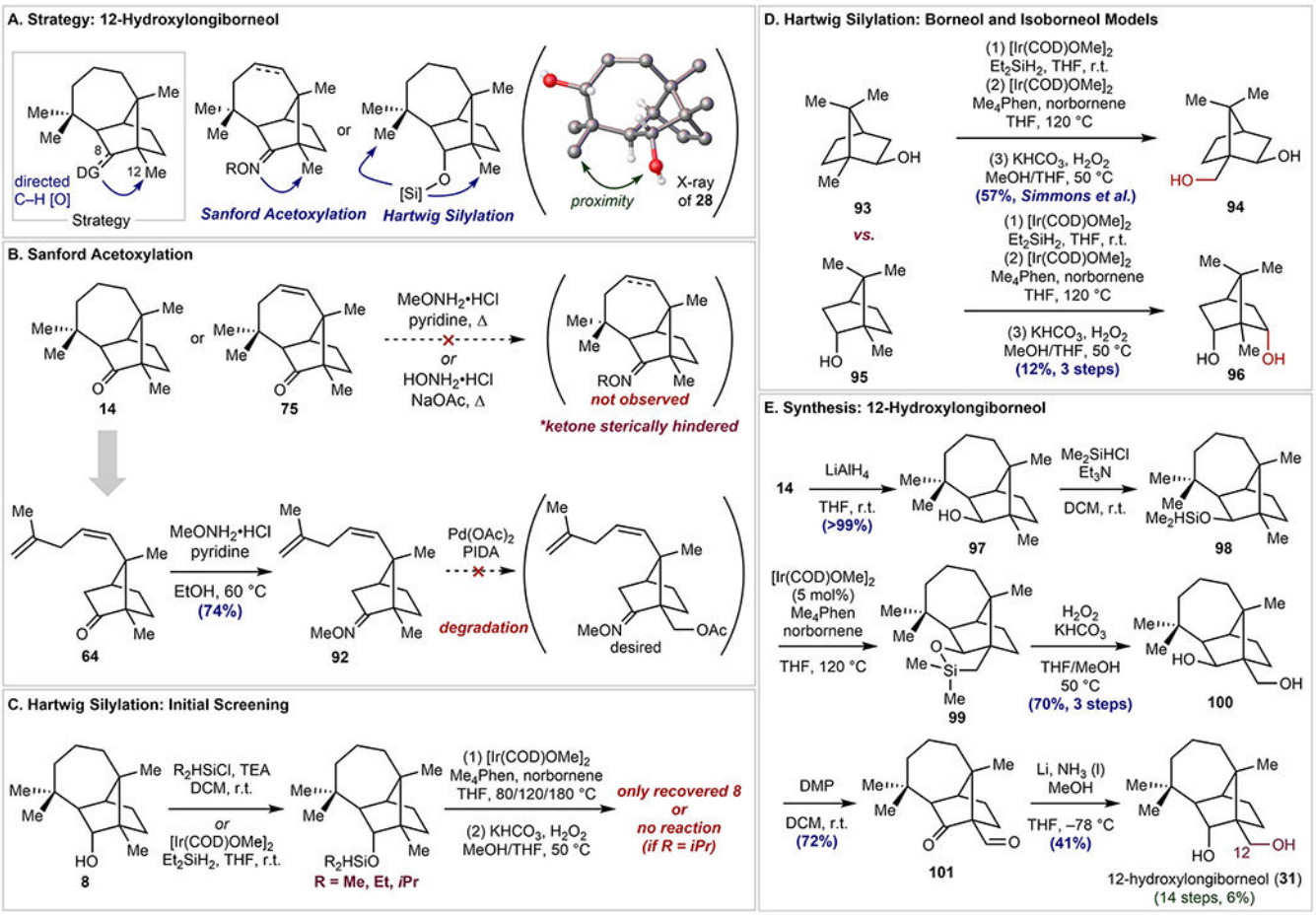

Figure 17.

(A) Oxygenation strategy for preparation of 12-hydroxylongiborneol (**31**). (B) Summary of methods attempted for oxime installation. (C) Attempted Hartwig silylations on longiborneol (**8**). (D) Hartwig silylations on isoborneol (**93**) and borneol (**95**) model systems. (E) Completed synthesis of 12-hydroxylongiborneol (**31**) based on insight from the model systems.

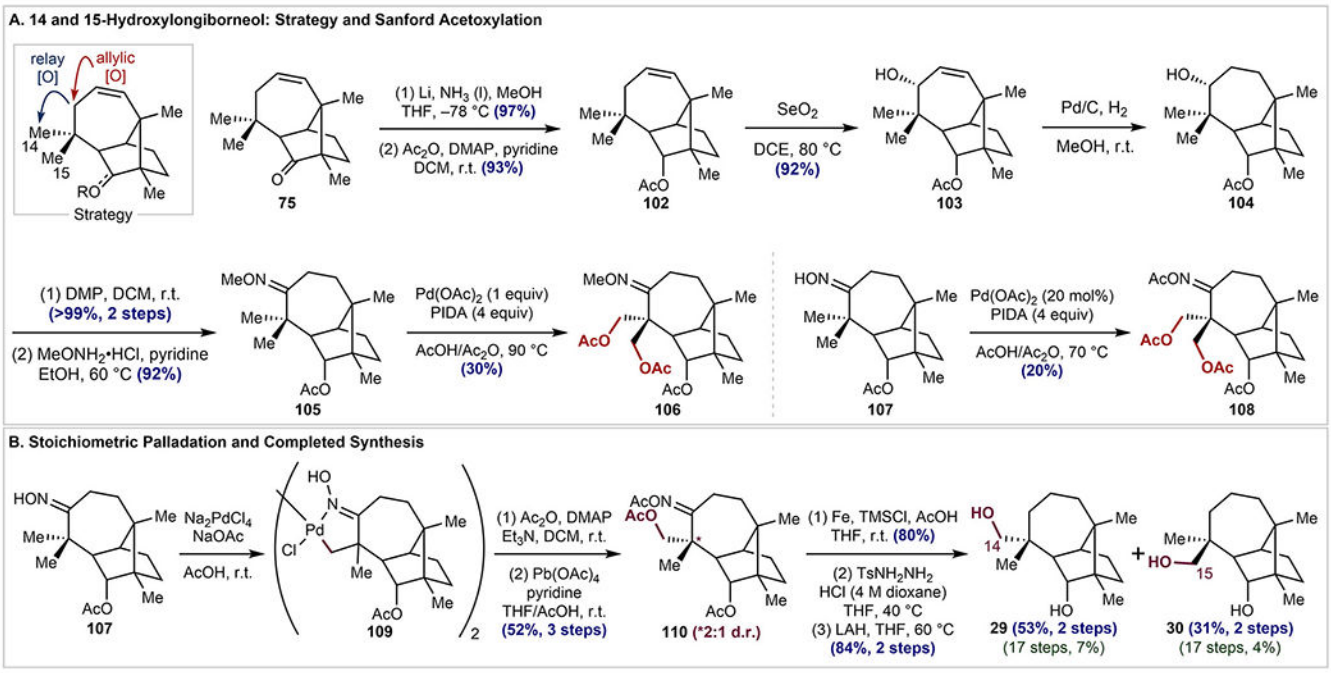

Figure 18.

(A) Revised oxygenation strategy for preparation of 14- and 15-hydroxylongiborneol (**29** and **30**). (B) Stoichiometric palladation then oxidation to prepare 14- and 15-hydroxylongiborneol (**29** and **30**).

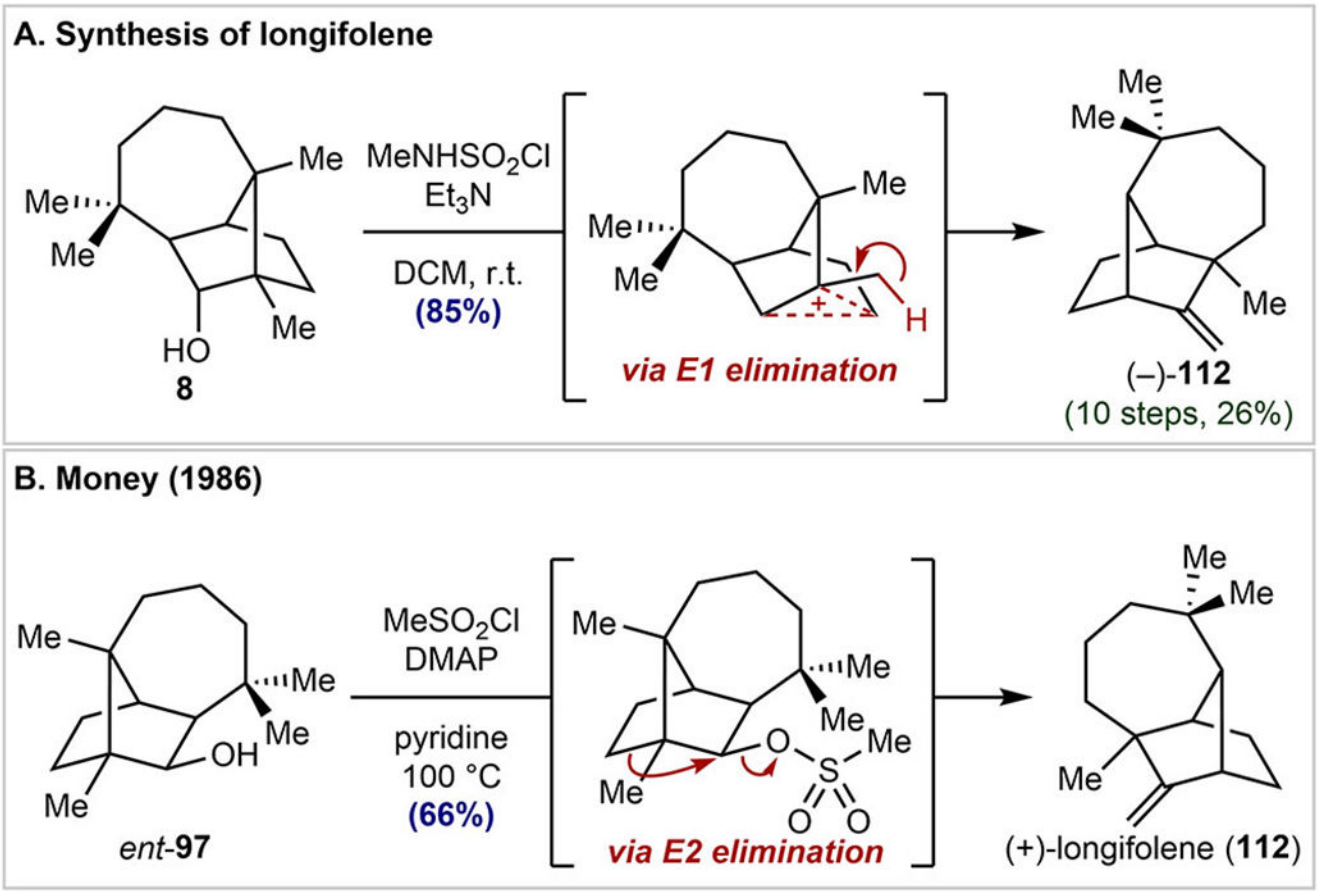

Figure 19.

(A) Rearrangement of longiborneol (**8**) to longifolene (**112**). (B) Related rearrangement observed by Kuo and Money[27] for the synthesis of **112**.

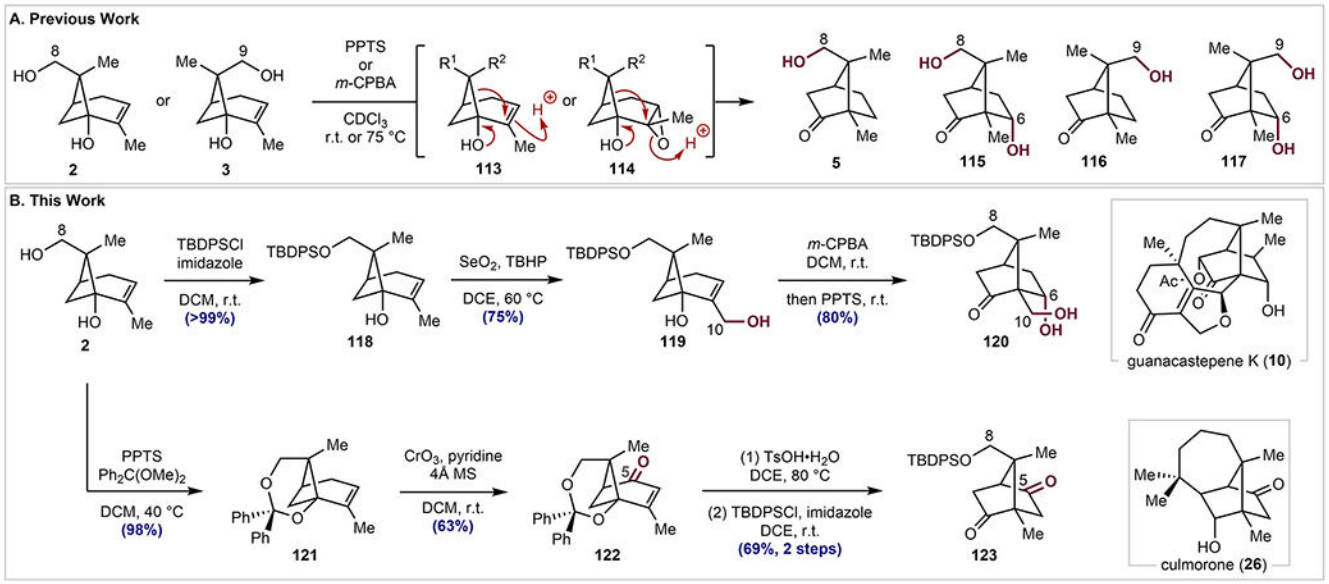

Figure 20.

(A) Our group's previous work on skeletal remodeling of carvone to camphor derivatives. (B) Synthesis of novel derivatives of camphor. With these, camphor derivatives functionalized at every nonactivated position of camphor can be produced from carvone.

Table 1.

Optimization of C–H Mono-acetoxylation

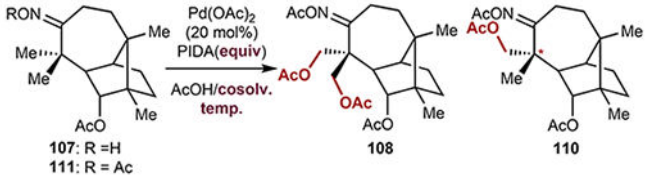

Entry	R	equiv PIDA	cosolvent	T (°C)	%yield 108:110	*d.r. (110)
1	H	4	Ac_2O	100	20% : 7%[a]	5.7:1
2	H	0.9	Ac_2O	100	9%[a] : 25%[a]	1.5:1
3	Ac	0.9	Ac_2O	100	11%[a] : 32%[a]	1.1:1
4	Ac	0.9	HFIP	30	trace : 25%[a]	1:1.2
5	Ac	0.9	Ac_2O	40	5%[a] : 33%[a]	2:1
6[b]	Ac	0.9	Ac_2O	40	4%[a] : 41%	2:1

[a]Yield by qNMR.

[b]26 mg scale.